Technical Report Documentation Page

1. Report No.	2. Government Accession No.	3. Recipient's Catalog No.
FHWA/TX-03/2100-P1		

4. Title and Subtitle	5. Report Date
ESTIMATING STRENGTH VERSUS LOCATION AND TIME IN HIGH-PLASTICITY CLAYS	February 2003
	6. Performing Organization Code

7. Author(s)	8. Performing Organization Report No.
Charles Aubeny and Robert Lytton	Product 2100-P1

9. Performing Organization Name and Address	10. Work Unit No. (TRAIS)
Texas Transportation Institute The Texas A&M University System College Station, Texas 77843-3135	11. Contract or Grant No. Project No. 0-2100

12. Sponsoring Agency Name and Address	13. Type of Report and Period Covered
Texas Department of Transportation Research and Technology Implementation Office P. O. Box 5080 Austin, Texas 78763-5080	Manual: September 2000-December 2002
	14. Sponsoring Agency Code

15. Supplementary Notes

Research performed in cooperation with the Texas Department of Transportation and the U.S. Department of Transportation, Federal Highway Administration

Research Project Title: Long-Term Strength Properties of High PI Clays Used in Embankment Construction

16. Abstract

Suction strongly influences the soil strength in slopes and earth structures constructed of high-plasticity clays. Strength degradation in earth structures can be explained in terms of moisture infiltrating into the soil mass, which reduces the suction and therefore strength of the soil. A moisture diffusion coefficient α controls the rate of moisture diffusion into a soil mass. Changes in suction during the life of a structure can be predicted from analytical and numerical solutions of the diffusion equation. This manual provides guidelines for predicting soil strength from estimated values of suction, estimating the moisture diffusion coefficient, and predicting suction as a function of location and time based on the estimated moisture diffusion coefficient. From these three steps, soil strength can be estimated as a function of location and time in slopes and earth structures.

17. Key Words	18. Distribution Statement
Clays, Slopes, Moisture Diffusion, Cracking, Earth Structures	No restrictions. This document is available to the public through NTIS: National Technical Information Service 5285 Port Royal Road Springfield, Virginia 22161

19. Security Classif.(of this report)	20. Security Classif.(of this page)	21. No. of Pages	22. Price
Unclassified	Unclassified	60	

Form DOT F 1700.7 (8-72) **Reproduction of completed page authoriz**

ESTIMATING STRENGTH VERSUS LOCATION AND TIME IN HIGH-PLASTICITY CLAYS

by

Charles Aubeny
Assistant Professor
Texas A&M University

and

Robert Lytton
Professor
Texas A&M University

Product 2100-P1
Project Number 0-2100
Research Project Title: Long-Term Strength Properties of High PI Clays
Used in Embankment Construction

Sponsored by the
Texas Department of Transportation
In Cooperation with the
U.S. Department of Transportation
Federal Highway Administration

February 2003

TEXAS TRANSPORTATION INSTITUTE
The Texas A&M University System
College Station, Texas 77843-3135

DISCLAIMER

The contents of this report reflect the views of the authors, who are responsible for the facts and the accuracy of the data presented herein. The contents do not necessarily reflect the official view or policies of the Federal Highway Administration (FHWA) or the Texas Department of Transportation (TxDOT). This report does not constitute a standard, specification, or regulation. The engineer in charge was Charles Aubeny, P.E., (Texas, # 85903).

ACKNOWLEDGMENTS

This project was conducted in cooperation with TxDOT and FHWA. The authors would like to express their appreciation to Project Director George Odom and Project Coordinator Mark McClelland, from the Texas Department of Transportation, for their support and assistance throughout this project.

TABLE OF CONTENTS

Page

List of Figures ..... **viii**
List of Tables ..... **ix**
Chapter 1: INTRODUCTION **1**
Chapter 2: SOIL SUCTION AND STRENGTH **3**
MATRIC, TOTAL, AND OSMOTIC SUCTION 3
UNITS OF SUCTION 4
RELATION BETWEEN SOIL SUCTION AND STRENGTH 5
EXAMPLE STRENGTH CALCULATIONS 7
Chapter 3: MOISTURE DIFFUSION THROUGH CLAY **9**
OVERVIEW 9
EVALUATION OF THE MOISTURE DIFFUSION COEFFICIENT 9
Correlation to Index Properties 10
Laboratory Evaluation 12
The Parameter (n) 19
Evaluation of α from Various Sources 19
Data Evaluation 20
Chapter 4: SLOPES **23**
ANALYTICAL PREDICTIONS 24
TIME TO FAILURE 27
Chapter 5: RETAINING STRUCTURES **29**
TYPICAL DESIGNS 29
BOUNDARY CONDITIONS 30
INITIAL CONDITIONS 32
MOISTURE DIFFUSION FOR TYPICAL SELECTED CASES 32
USE OF SUCTION PREDICTION ANALYSES 46
References **49**

LIST OF FIGURES

Page

Figure 1. The pF Suction Scale. 5
Figure 2. Empirical Correlations of Index Properties to Clay Permeability. 11
Figure 3. Dry End Test for Measuring α. 12
Figure 4. Analytical Solution for Dry End Test. 16
Figure 5. Typical Dry End Test Results 17
Figure 6. Matric Suction Versus Time in Intact and Cracked Slope Surfaces. 25
Figure 7. Definition Sketch for Moisture Diffusion into Intact Slope. 26
Figure 8. Definition Sketch for Moisture Diffusion into Cracked Slope. 26
Figure 9. Typical TxDOT Earth Retaining Structure. 29
Figure 10. Boundary and Initial Suctions for Moisture Diffusion Analyses. 31
Figure 11. Definition Sketch for Suction Predictions. 33
Figure 12. Suction versus Time for Structure with Aspect Ratio 4H:1V and U_0=5. 34
Figure 13. Suction versus Time for Structure with Aspect Ratio 4H:1V and U_0=4. 35
Figure 14. Suction versus Time for Structure with Aspect Ratio 4H:1V and U_0=3. 36
Figure 15. Suction versus Time for Structure with Aspect Ratio 4H:1V and U_0=2. 37
Figure 16. Suction versus Time for Structure with Aspect Ratio 4H:1V and U_0=1. 38
Figure 17. Suction versus Time for Structure with Aspect Ratio 4H:1V and U_0=0.5. 39
Figure 18. Suction versus Time for Structure with Aspect Ratio 8H:1V and U_0=5. 40
Figure 19. Suction versus Time for Structure with Aspect Ratio 8H:1V and U_0=4. 41
Figure 20. Suction versus Time for Structure with Aspect Ratio 8H:1V and U_0=3. 42
Figure 21. Suction versus Time for Structure with Aspect Ratio 8H:1V and U_0=2. 43
Figure 22. Suction versus Time for Structure with Aspect Ratio 8H:1V and U_0=1. 44
Figure 23. Suction versus Time for Structure with Aspect Ratio 8H:1V and U_0=0.5. 45

LIST OF TABLES

Page

Table 1. Soil Sample Index – Waco Site. 17
Table 2. Summary of Moisture Diffusion Tests. 18
Table 3. Moisture Diffusion Coefficient α from Different Sources 19
Table 4. Diffusion Coefficients Inferred from Paris Clay Slope Failure Data (11) 21
Table 5. Diffusion Coefficients Inferred from Beaumont Clay Slope Failure Data (11) 22

CHAPTER 1:
INTRODUCTION

High-plasticity clays occur in many areas of Texas and often offer the most economical material alternative for construction of highway embankments. When constructed with proper moisture and compaction control, embankments constructed of plastic clays can perform adequately with regard to overall stability. However, experience shows that the outer layers of these embankments can experience dramatic strength loss. Softening of the surficial soils can begin soon after construction and continue for decades. The consequent sloughing and shallow slide failures represent a significant maintenance problem for TxDOT. The problem of strength loss in high plasticity clay soils can also impact other structures such as retaining walls, pavements, and riprap. This manual provides guidelines for estimating soil strength loss as a function of time and space for typical slopes and earth structures used in TxDOT projects.

The soils in the slopes and earth structures described above are unsaturated. Accordingly, soil suction contributes substantially to the shear strength of the soil, and changes in soil strength can largely be attributed to changes in suction. The magnitude of soil suction in clayey soils compacted at or near the optimum moisture content is typically high – on the order of u=4 pF with a correspondingly high shear strength. Over time moisture can migrate into the earthfill, with a concomitant decrease in the magnitude of suction and strength. The amount of strength loss will depend on environmental moisture conditions, while the rate of strength loss will be governed by the moisture diffusion properties of the soil.

Since suction plays a pivotal role in the process described above, Chapter 2 of this manual presents basic principles of suction and its relationship to shear strength of unsaturated soils. This manual presents methods of predicting soil suction in slopes and earth structures based on knowledge of simple soil index properties and environmental moisture conditions without need for direct measurements of soil suction.

As mentioned earlier, the time rate and spatial extent of soil shear strength degradation in a slope or earth structure will be controlled by (1) the moisture diffusion properties of the soil, and (2) the moisture and suction conditions existing on the boundaries of the soil mass under consideration. A moisture diffusion coefficient (designated as α in this report) that can be either directly measured in a simple laboratory test or estimated from grain size and consistency limit data characterizes the moisture diffusion properties. Chapter 3 describes these methods.

Chapter 4 addresses suction loss and strength degradation due to moisture infiltration in slopes. The basic issue addressed with regard to slopes is the effectiveness of various design measures in delaying or avoiding shallow slide problems. Two types of designs are considered: vegetative and concrete riprap slope protection. In this chapter, analytical predictions compare the rate of strength degradation for these two types of slope protection. The primary variable controlling the times at which slope failure can occur is the moisture diffusion coefficient discussed in Chapter 3.

Chapter 5 addresses the issue of strength loss in earth-retaining structures. Strength degradation in these structures is dependent upon a number of parameters in addition to the moisture diffusion properties of the soil including the moisture, suction at the boundaries of the retaining structure, and suction levels in local subgrade soils. Given this variety of parameters, a single analytical prediction of strength loss is not possible. Therefore a series of parametric studies are presented covering a realistic range of soil and site conditions.

CHAPTER 2:
SOIL SUCTION AND STRENGTH

Changes in soil suction over time play a critical role in strength degradation in soils during the life of a slope or earth structure. Accordingly it is important for a designer of these structures to understand basis concepts of suction and how suction relates to shear strength of the soil. The following sections of this chapter present these basic concepts.

MATRIC, TOTAL, AND OSMOTIC SUCTION

Surface tension at the air-water interface in an unsaturated soil will lead to negative water pressures in the soil referred to as matric suction. This negative pressure directly affects the intergranular stresses between soil particles and therefore has a strong influence on soil strength. Higher magnitudes of suction bind the soil particles more tightly together leading to higher soil strength. While suction always represents a negative water pressure, some authors and references adopt a sign convention in which suction is a positive number. Provided one is consistent, such a convention can lead to correct results. However, regardless of the sign convention used, it is important for the soils engineer to remember that under the usual field conditions in which the air phase is at atmospheric pressure, the water pressure in a partly saturated soil is physically a negative value.

Matric suction in a soil varies with the soil's moisture content. The relation between matric suction and moisture is referred to as the soil-moisture characteristic curve. Since the soil moisture content typically varies during the life of an earth structure, it follows that suction will also vary. As the soil moistens matric suction and soil strength will decline, and vice-versa. The laws governing the diffusion of moisture into and out of an unsaturated soil mass parallel in many ways those for saturated soils with which most geotechnical engineers are familiar. Hence, changes in matric suction over time in a slope or earth structure are governed by predictable processes of moisture diffusion through soils.

Gradients of total suction drive moisture flow through unsaturated soils. Matric suction is one component of total suction. However, there is another component of total suction that will influence moisture flow: osmotic suction. Osmotic suction relates to the tendency of water molecules to migrate from a region of low salt concentration to that of a higher concentration. The total suction (h_t) in a soil is the sum of osmotic suction (π) and matric suction (h_m):

$$h_t = \pi + h_m \quad \text{(Eq. 1)}$$

When working with suction, one must remember that moisture flow calculations must be in terms of total suction, while soil strength and deformation calculations must be in terms of matric suction.

UNITS OF SUCTION

Suction can be expressed in the usual units of water pressure; e.g., pounds per square foot (psf) or head of water (ft). An alternative widely used measure of suction is the pF scale, expressed as the logarithm of the head in centimeters (cm) of water:

$$u(pF) = \log_{10} [-h(cm)] \quad \text{(Eq. 2)}$$

Figure 1 shows several important reference points on the pF scale for total suction. Two particularly noteworthy reference points are the wet limit for clays and the wilting point, which are pF 2.5 and 4.5, respectively. These points are important since they define the lower and upper range of suction in clays that will occur in most field situations. More specific ranges associated with climactic regions of Texas will be presented later in this report. However, the reference points shown in Figure 1 provide a good initial guide as to what levels of suction can occur in clay soils.

The mathematical analysis of moisture flow through unsaturated soils is considerably simplified when suction is expressed on a logarithmic (pF) scale rather than a natural scale. For this reason predictions of suction over time within a soil mass are presented in terms of a pF scale in this manual. For strength calculations, analyses must convert suction on a pF scale to units of pressure making use of Eq. 2.

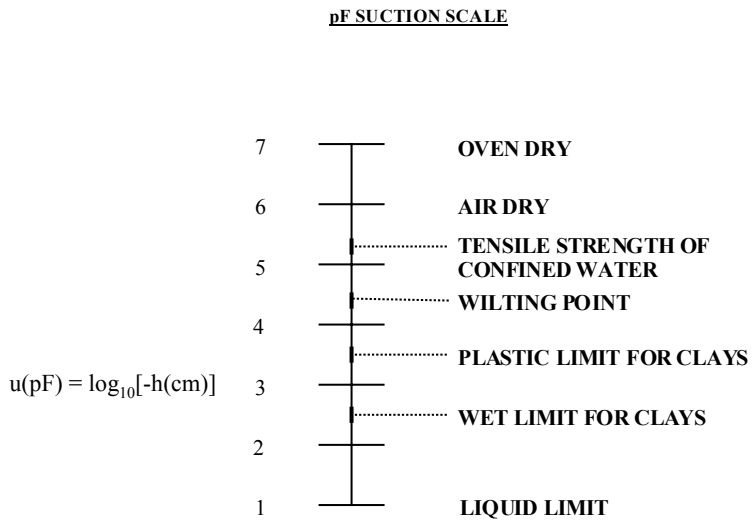

Figure 1. The pF Suction Scale.

RELATION BETWEEN SOIL SUCTION AND STRENGTH

Assuming a condition of no excess pressure in the pore-air phase - a reasonable assumption when considering long-term strength - the shear strength of an unsaturated soil can be characterized by a Mohr-Coulomb relationship of the form:

$$\tau_f = c_{app} + \sigma' \tan \phi' \qquad \text{(Eq. 3a)}$$

where: σ' = net mechanical stress
ϕ' = mechanical stress internal friction angle
τ_f = failure shear stress

The apparent cohesion (c_{app}) in Eq. 3a is defined by:

$$c_{app} = - h_m \; f \Theta \tan \phi' \qquad \text{(Eq. 3b)}$$

where: ϕ' = mechanical stress internal friction angle
Θ = volumetric water content (volume water/total volume)
f = factor ranging from f=1 to f=1/Θ

Computation of strength using Eq. 3 is most expedient in cases for which an effective stress analysis is to be performed, typically in cases where the net mechanical stress contributes

substantially to the shearing resistance. In problems involving shallow soils for which the soil shear strength is dominated by suction, it is often useful to characterize soil strength in terms of an unconfined shear strength (C_{uc}). If the matric suction (h_m) is known or has been estimated, the following expression characterizes the unconfined shear strength:

$$C_{uc} = - h_m \; f \Theta \sin \phi' / [1 - \sin \phi'] \qquad \text{(Eq. 4a)}$$

where ϕ', Θ, and f are as defined in Eq. 3. Eq. 4a is valid so long as all excess pore pressures generated during shearing have dissipated. This is generally a valid assumption when considering the long-term stability of slopes and earth structures. However, as full saturation is approached during wetting of a soil, strains may develop relatively rapidly due to the final stages of softening of the soil, in which load-induced pore pressures may be generated. In this case, a lower bound (undrained) estimate of the unconfined compressive shear strength is:

$$C_{uc} = - h_m \; f \Theta \sin \phi' / [1 - (1 - a_f) \sin \phi'] \qquad \text{(Eq. 4b)}$$

where: a_f = is the Henkel pore pressure coefficient at failure.

A typical value of Henkel's coefficient (a_f) for a compacted soil wetted to saturation is about 1.4. A significant advantage of characterizing soil strength in terms of the unconfined compressive strength (Eq. 4) is that the effects of load-induced pore pressures (characterized by a_f) are readily incorporated into the strength estimate.

Both Eqs. 3 and 4 require an estimate of the mechanical stress friction angle. This can be directly measured in the laboratory, typically in a consolidated-undrained triaxial shear test with pore pressure measurements. However, the friction angle can often be satisfactorily estimated using an empirical correlation to the plasticity index *(1)*:

$$\sin \phi' = 0.8 - 0.22 \log_{10} (PI) \qquad \text{(Eq. 5)}$$

The factor (f) in Eqs. 3 and 4 accounts for the fact that in an unsaturated soil the water phase does not act over the entire surface of the soil particles *(2)*. For degrees of saturation less than S<85 percent, f is essentially equal to unity. As full saturation is approached f=1/Θ. For degrees of saturation intermediate between these cases, 85 percent<S<100 percent, f can be

reasonably estimated by linear interpolation. This behavior can be expressed in equation form as follows:

$$S = 100\,\text{percent} \qquad f = 1/\Theta \qquad \text{(Eq. 6)}$$
$$S \le 85\,\text{percent} \qquad f = 1$$
$$85\,\text{percent} < S < 100\,\text{percent} \qquad f = 1 + \frac{S - 85}{15}\left(\frac{1}{\Theta} - 1\right)$$

EXAMPLE STRENGTH CALCULATIONS

A high plasticity clay is compacted to a dry density (γ_d) of 93 pcf with a matric suction (u) 4.0pF, and a moisture content w=22 percent. The specific gravity (G_s) and friction angle (ϕ') are estimated to be 2.70 and 26 degrees, respectively. Compute the unconfined compressive strength C_u (Eq. 4) for the following conditions: as compacted with u=4 pF, after saturation to u=2 pF, and at an intermediate wetting stage with u=3.0 pF.

a. As-compacted strength:

The first step is to determine the degree of saturation of the as-compacted material. This can be done by first computing the void ratio (e) of the soil:

$e = (G_s\,\gamma_w / \gamma_d) - 1 = (2.70 \times 62.4\text{ pcf} / 93\text{ pcf}) - 1 = 0.81$

The corresponding degree of saturation (S) is computed from:

$S = w\,G_s / e = (0.22)(2.70) / 0.81 = 73.3$ percent.

Since the degree of saturation (S) is less than 85 percent, f=1.0.

The volumetric water content Θ is:

$\Theta = w\,(\gamma_d / \gamma_w) = 0.22 \times (93\text{ pcf}/62.4\text{ pcf}) = 32.8$ percent

A matric suction u=4pF corresponds to $h_m = -10^4$ cm of water or -20,500 psf. Applying f, Θ, h_m, and ϕ' in Eq. 4 yields:

$C_u = (20{,}500\text{ psf})\,(1.0)\,(0.328)\,\sin 26^o / (1 - \sin 26^o) = 5250$ psf

b. Saturated strength

Since the saturation (S) is 100 percent, $f = 1/\Theta$, or $f\,\Theta = 1$. The matric suction in units of pressure is -100 cm of water or -205 psf. Substitution in Eq. 4 results in the following apparent cohesion assuming no generation of excess pore pressures due to loading:

$C_u = (205\text{ psf})\,(1.0)\,\sin 26^o / (1 - \sin 26^o) = 160$ psf

If excess pore pressures are assumed to develop with a Henkel pore pressure coefficient (a_f) of 0.7, the apparent cohesion becomes:

C_u = (205 psf) (1.0) sin 26^o/ [1- (1 - 0.7) sin 26^o] = 100 psf

c. Strength at u = 3.0pF

To estimate strength, one must first make an estimate of the water content (w) and degree of saturation at the suction level in question. For matric suctions in the range u=2 to 4 pF, a reasonable assumption is that the water content varies linearly with suction on a pF scale. The moisture content calculations are therefore as follows:

Matric suction, u	Moisture Content (w)
4 pF	22 percent (given at start of problem)
2 pF	$w_{sat} = e/G_s$ = 30.7 percent

The moisture content at u=3.0 pF can now be estimated by interpolation:

$w_{3.0}$ = 30.7 + [(22-30.7) / (4-2)] (3.0-2.0) = 26.3 percent

The corresponding degree of saturation (S) is computed from:

S = w G_s / e = (0.263)(2.70) / 0.81 = 87.7 percent

The volumetric water content Θ is:

Θ = w (γ_w / γ_d) = 0.263 x (93pcf/62.4pcf) = 39.2 percent

Since the degree of saturation is between 85 and 100 percent, f must be estimated by interpolation. Recalling than when S=85 percent f=1 and when S=100 percent f=1/Θ, the appropriate interpolation is:

f = 1 + [(87.7-85) / (100-85)] (1 / 0.392 - 1) = 1.28.

For a matric suction u=3.0 pF = -1,000 cm water = -2050 psf, the apparent cohesive strength can now be estimated from Eq. 4:

C_u = (2050 psf) (1.28) (0.392) sin 26^o/ (1- sin 26^o) = 800 psf

Finally, one should note that the volumetric calculations above are based on a constant void ratio (e). In actuality, changes in void ratio will occur with changes in suction. However, the effect is small compared with other variables in the problem. In particular, one should recall that during the wetting process the magnitude of matric suction declines from 20,500 psf to 205 psf. Given this enormous variation in the scale of suction, secondary effects associated with void ratio changes can be reasonably neglected in the strength calculations.

CHAPTER 3:
MOISTURE DIFFUSION THROUGH CLAY

OVERVIEW

Chapter 2 of this manual presents basic concepts regarding suction and connects suction to soil strength. As noted in that chapter, suction will change over time at various locations within a soil mass as moisture content changes occur in the mass. A process of moisture diffusion governs these suction and moisture content changes. A rational analysis of the moisture diffusion process requires knowledge of the moisture diffusion properties of the soil, the moisture-suction conditions on the boundaries of the soil mass, and the geometry of the soil mass. The first item will be considered in this chapter.

EVALUATION OF THE MOISTURE DIFFUSION COEFFICIENT

The relationship governing moisture diffusion through an unsaturated soil is the following partial differential equation *(3)*:

$$\nabla^2 u = \frac{1}{\alpha}\frac{\partial u}{\partial t} \qquad \text{(Eq. 7)}$$

where u = total suction on a pF scale
t = time
α = a moisture diffusion coefficient

Knowledge of partial differential equations is not needed for using this manual, since solutions to Eq. 7 for various boundary conditions are provided in Chapters 4 and 5. However, the equation is presented here to emphasize two points. First, the most convenient form of the equation is suction expressed on a logarithmic (pF) scale. Second, a single material parameter, the moisture diffusion coefficient (α), controls the rate of moisture migration through an unsaturated soil mass. The coefficient α is analogous to the coefficient of consolidation (c_v) in saturated soil mechanics. In fact, both parameters have the same units, the square of length per unit time, such as feet squared per year (ft^2/yr) or centimeters squared per second (cm^2/sec).

The moisture diffusion coefficient (α) can be measured directly by monitoring changes in suction in a sample of undisturbed soil subjected to a suction gradient. However, in many instances satisfactory estimates of α can be based on empirical correlations to index properties. The following sections present both approaches.

Correlation to Index Properties

The moisture diffusion coefficient (α) can be expressed in terms of several soil parameters as follows:

$$\alpha = |S|\ p\ \gamma_w / \gamma_d \qquad \text{(Eq. 8)}$$

where γ_d = dry unit weight of soil

γ_w = unit weight of water

$|S|$ = slope of the pF versus gravimetric water content line

The parameter p is determined from:

p = a measure of unsaturated permeability = $|h_0|\ k_0 / 0.434$

k_0 = the saturated permeability of the soil

$|h_0|$ = the suction at which the soil saturates, approximately 200 cm

The parameter S can be obtained from the soil moisture characteristic curve, which is commonly measured with a pressure plate apparatus. If such data are not available, Texas Transportation Institute (TTI) Project Report 197-28 presents the following empirical relationship *(4)*:

$$S = -20.29 + 0.155\ (LL) - 0.117\ (PI) + 0.0684\ (\text{percent Fines}) \qquad \text{(Eq. 9)}$$

where LL is the liquid limit, PI is plasticity index, and percent Fines is the percentage of particle sizes passing the No. 200 sieve on a dry weight basis.

Likewise the saturated permeability (k_0) can be measured directly in laboratory permeability or consolidation tests. Empirical correlations can also provide reasonable estimates of saturated permeability in clays. For example, Figure 2 presents estimates of saturated permeability as a function of void ratio (e), plasticity index (PI), and clay fraction (CF) *(5)*. The clay fraction (i.e., the percentage of particle sizes finer than 2 microns) can be measured from a conventional hydrometer test. The correlations in Figure 2 do not extend to permeability values below about $3x10^{-9}$ cm/sec. Permeability values less than this value are actually unlikely in the field, since cracking is likely to occur in such soils. Hence, extrapolation of the curves to values less than $3x10^{-9}$ cm/sec is not recommended. If the data plot to the left of this value, a saturated permeability (k_0) value of $3x10^{-9}$ cm/sec is recommended.

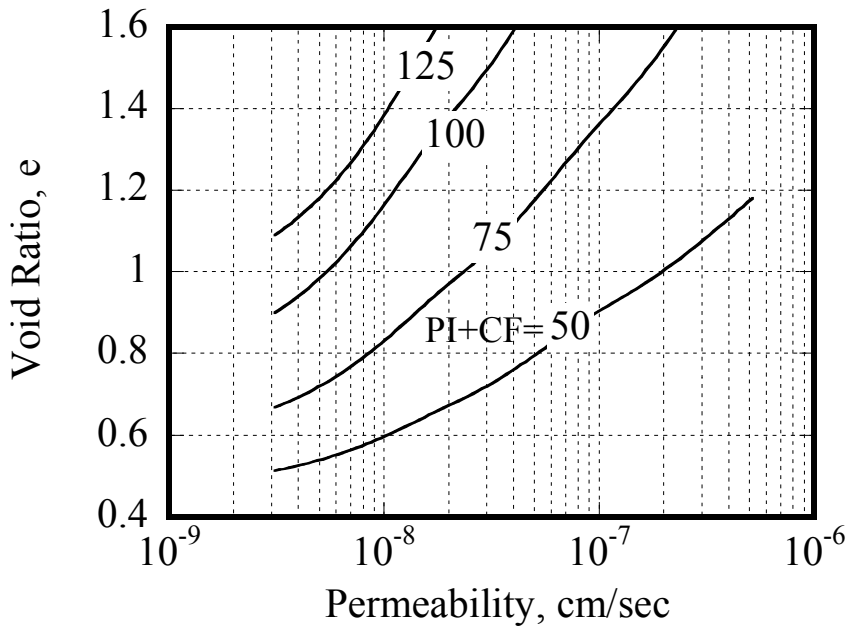

Figure 2. Empirical Correlations of Index Properties to Clay Permeability. Source: Tavenas et al. (*5*)

Design of shallow foundations on expansive clays also requires estimates of the diffusion coefficient (α), and empirical correlations based on soil index properties can be found in the expansive clay literature. Empirical estimates of α are embodied into the expansive clay design procedure developed by Covar and Lytton *(6)*. Information from this source can provide a

valuable supplement to estimates based on Eq. 8 or to direct laboratory measurements that will be described subsequently.

Laboratory Evaluation

To evaluate the diffusion coefficient (α) in the laboratory, Mitchell *(3)* proposed two tests that could be performed on conventional undisturbed soil samples, such as Shelby tube samples. In both tests, the sides and one end of the sample are sealed as shown in Figure 3. The other end of the sample is left open to permit the flow of moisture into or out of the sample as will be discussed subsequently. Small holes are drilled into the sides of the sample at several locations, and psychrometers are installed for measuring suction. For the recent tests performed at Texas A&M University (TAMU), six thermocouple psychrometers were installed; however, the results of the test program indicated that one or two psychrometers nearest the open end of the specimen are actually sufficient for obtaining reliable estimates of α *(7)*.

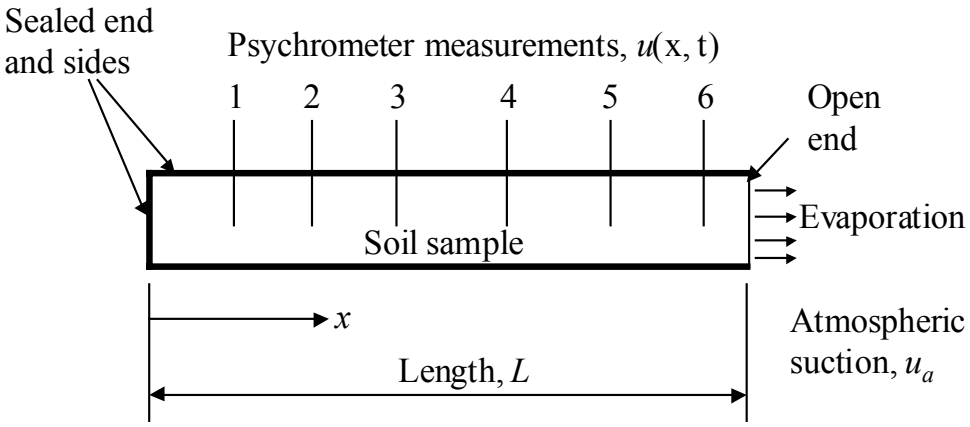

Figure 3. Dry End Test for Measuring α.

Different tests are possible by controlling the suction boundary at the open end of the sample; namely, "wetting" and "drying" tests are possible (*3*). The TAMU tests employed the drying procedure with satisfactory results; hence, this manual will present that procedure. The test involves sealing all boundaries of a cylindrical specimen except for one end that is exposed to the atmosphere. Except for extremely dry soils, the relative humidity in the soil typically

exceeds 99 percent while that of the atmosphere is about 50 percent; hence, exposure of the open end to air will cause moisture to flow out of the soil at the open boundary.

Equipment and Procedures

The dry end test proceeds according to the following steps:

1. Suction in the soil is measured with wire-screen thermocouple psychrometers, which measure total suction by measuring the relative humidity of the air phase in a soil (*8*). The output signal of these psychrometers is measured in millivolts, which can be calibrated to suction by inserting the probes in sealed containers containing air-water solutions with varying salt concentrations in the water. In this case, the solutions contained sodium chloride (NaCl) concentrations corresponding to osmotic suctions of pF 3.6, 4.0, and 4.5. Psychrometers are generally capable of obtaining measurements over a soil suction range of about pF 3.0 to 4.5, which in general proved adequate for the soil specimens tested in this experimental program. The accuracy of the calibration is very important, so the calibration measurements should be repeated until satisfactory reliability is ensured.
2. Six holes are drilled to approximately one-half the sample diameter at roughly equally spaced intervals for insertion of the suction measurement probes. The hole diameters must be sufficient to permit insertion of the psychrometer but create minimal air space between the soil and psychrometers.
3. The sample is wrapped with a double layer of aluminum foil to seal all boundaries of the specimen. Locations at which the wires leading to the suction probes penetrated the external plastic wrap and aluminum foil required special attention, as these provided possible conduits for moisture loss through the sides of the soil specimen. Silicon sealant and electrical tape were applied at these locations to minimize the potential for moisture loss.
4. The relative humidity (*RH)* in the ambient air in the laboratory is measured with a sling psychrometer (*9*) comprised of a wet bulb thermometer that measures the adiabatic saturation temperature, T_{wb}, and a dry bulb thermometer that simply measures the air temperature, T_{db}. The two thermometers are mounted on a common swivel and are rotated to ensure sufficient airflow around the wet bulb. The measured temperatures, T_{wb} and T_{db}, are used with psychrometric charts to estimate relative humidity, *RH*.

5. To start the test, the foil is removed from one end of the specimen. Electrical tape is applied to the foil-soil interface at the open end to ensure a proper seal at this boundary. During the test, drying near the open end of the specimen induced shrinkage in the specimen with a corresponding tendency of the soil to pull away from the external seal. The test operator counteracted this effect by periodically tightening the foil wrap at the open end throughout the duration of the test.
6. After an initial set of psychrometer readings is taken to establish the initial suction (u_0) in the specimen, follow-up readings are taken at about 2-hour intervals to monitor changes in suction as drying occurs. Depending on the rate of drying, the duration of the test must be from one to three days to obtain sufficient changes in suction for meaningful estimates of α.

Data Interpretation

Interpretation of measured data is as follows:

1. The total suction in the atmosphere on the boundary of the specimen, h_a in feet, is computed from relative humidity measured by the sling psychrometer as follows:

$$h_a \text{ (cm)} = 10{,}811 \text{ (T+273.16) } \log_{10} \text{ (RH/100)} \qquad \text{(Eq. 10)}$$

where h_a = atmospheric total suction in cm
T = temperature in degrees centigrade
RH = relative humidity in percent

The drying test must be interpreted entirely in terms of suction in pF, so the head computed from Eq. 10 must be converted to pF using Eq. 2 to obtain u_a.

2. Make an initial estimate of α to compute the theoretical value of the suction corresponding to each measurement location x and measurement time t using the expression developed by Mitchell (*3*):

$$u = u_a + \sum_{n=1}^{\infty} \frac{2(u_0 - u_a)\sin z_n}{z_n + \sin z_n \cos z_n} \exp\left[\frac{z_n^2 \alpha t}{l^2}\right] \cos\left[\frac{z_n x}{l}\right] \qquad \text{(Eq.11)}$$

$$\cot z_n = z_n / h_e L$$

where u_a = atmospheric suction

u_0 = initial suction in soil

α = diffusion coefficient

t = time

L = sample length

x = psychrometer coordinate

h_e = evaporation coefficient (estimate $h_e = 0.54 cm^{-1}$)

3. Compute the difference (E) between the theoretical value of suction (u_{theory}) predicted from Eq. 11 and suction measured by the psychrometers ($u_{measured}$):

$$E = u_{theory} - u_{measured} \quad \text{(Eq.12)}$$

4. Sum the square of the errors E_{sum} for all measurements:

$$E_{sum} = \Sigma (u_{theory} - u_{measured})^2 \quad \text{(Eq.13)}$$

5. Optimize α to minimize the E_{sum} in Step 4. This step can be performed by user employing a trial and error approach or by using optimization algorithms included with most spreadsheet programs.

Hand calculation of Eq. 11 is in general not practical, although programming of this equation on most personal computers is relatively straightforward. As an aid to checking calculations, Figure 4 presents Eq. 11 graphically for a somewhat typical case of the product of the evaporation coefficient times the specimen length (h_e x L) equaling 22. In principle, other values of h_e x L will affect the solution, and Eq. 11 should be re-computed for each individual case. However, experience to date has shown that minor variations in this product do not have a great influence on interpreted α values. Hence, the solution shown in Figure 4 can be used for interpreting moisture diffusion test data if computer facilities are unavailable.

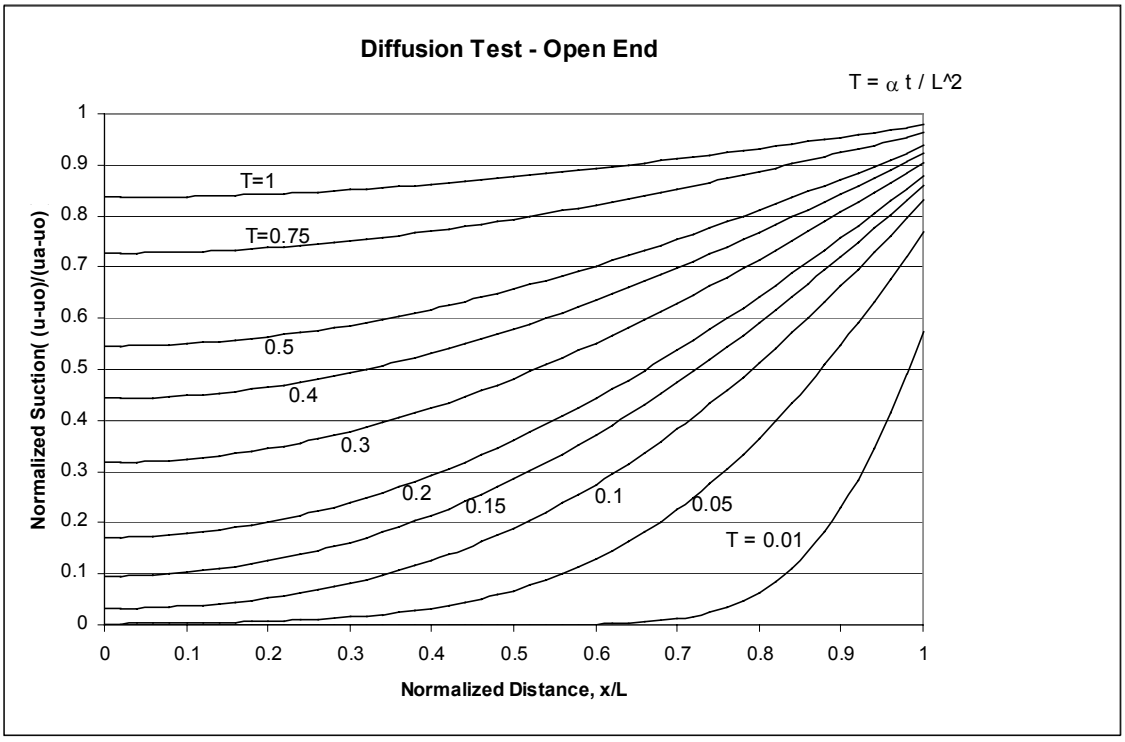

Figure 4. Analytical Solution for Dry End Test.

Figure 5 shows typical test results for a dry end test. A total of nine dry end moisture diffusion tests were performed on the high plasticity clay samples described in Table 1. The soils had properties of a high-plasticity clay (CH): liquid limits (LL) of 56-66, plasticity indices of 34-44, a fine fraction (passing the #200 sieve) of 56-92 percent, and a clay fraction of 40 percent. All samples were comprised of 3-inch diameter tube samples obtained at relatively shallow depths (2 to 16 ft) from compacted clay highway embankments. The length of the specimens used in the experiments varied somewhat depending on the length of intact soil in the tube samples; typical lengths varied from 0.6 to 0.95 ft. The samples as received from the field had already been extruded from the sampling tubes and were wrapped in plastic wrap. The samples were stored in a controlled humidity and temperature environment prior to testing.

The moisture diffusion tests are summarized in Table 2. Eight of the nine tests were judged successful. One test, Test 8, failed due to failure of the psychrometer measurement devices during the test. In general, the psychrometer located near the open end of the specimen provided the most reliable estimates of α, since it experienced the largest changes in suction. Two data points (Test 1, Psychrometer 5 and Test 9, Psychrometer 5) appeared to be somewhat anomolous and were therefore excluded from statistical calculations. The tests judged as most

reliable yielded an average moisture diffusion coefficient $\alpha = 3.1 \times 10^{-5}$ cm^2/sec with a standard deviation of 1.2×10^{-5} cm^2/sec.

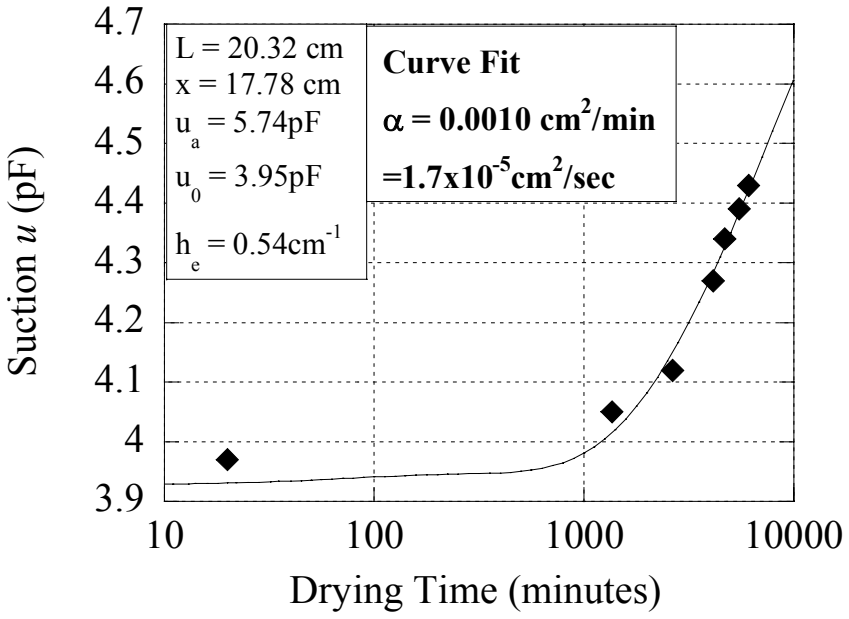

Figure 5. Typical Dry End Test Results.

Table 1. Soil Sample Index – Waco Site.

Sample	Depth	Description
1	8-10 ft	Light brown fat clay with coarse to medium sand, roots, maximum particle size coarse sand (CH)
2	6-8 ft	Orange-brown fat clay, with coarse sand and gravel, roots, maximum particle size gravel (CH)
3	12-14 ft	Medium brown fat clay with medium sand, roots, maximum particle size coarse sand (CH)
4	2-4 ft	Dark brown fat clay, with coarse sand and gravel, maximum particle size gravel (CH)
5	2-4 ft	Dark brown lean clay with coarse sand and gravel, roots, maximum particle size gravel (CL)

Table 2. Summary of Moisture Diffusion Tests.

Test	Sample Length (ft)	Measurement Location* (ft)	Initial Suction (pF)	Boundary Suction (pF)	Diffusion Coefficient (10^{-5} cm^2/sec)
1	0.958	0.708	3.39	5.64	7.7**
		0.833	4.20	5.64	3.0
2	0.792	0.458	3.30	5.83	4.0
		0.583	3.45	5.83	5.0
3	0.729	0.438	2.60	5.80	4.0
		0.542	3.20	5.80	1.5
		0.646	3.9	5.80	2.0
4	0.688	0.396	3.60	5.91	2.3
		0.500	3.80	5.91	2.2
		0.604	3.80	5.91	3.7
5	0.667	0.583	3.95	5.74	1.7
6	0.625	0.450	3.75	6.00	3.2
		0.542	4.10	6.00	1.3
7	0.700	0.521	3.40	5.62	4.2
		0.617	3.70	5.62	4.7
8	***	***	***	***	***
9	0.750	0.667	3.25	5.93	8.3**

*Measured from sealed end of specimen.

**Data points excluded from average.

***Failed Test.

The Parameter (n)

The analytical framework for evaluating moisture diffusion through unsaturated soil is based on an assumed simple inverse relationship between unsaturated permeability and matric suction; i.e., $k/k_0 = h_0/h$. For cases in which permeability actually varies inversely with a higher power of suction, i.e., $k/k_0 = h_0/h^n$ where $n>1$, Aubeny and Lytton present a method for generalizing the analysis *(7)*. However, Table 2 shows that in most cases assuming n=1 provides the best fit between theory and measurement for high plasticity clays. Therefore, subsequent analyses in this manual will be based on n=1.

Evaluation of α from Various Sources

The TAMU laboratory diffusion coefficient measurements in Table 2 were evaluated through comparison to a number of sources including: Mitchell's experience with high plasticity Australian clays *(3)*, the empirical relations (Eq. 8, Eq. 9, and Figure 2) presented earlier, and back-calculation of slope failures in Paris and Beaumont clays. Table 3 summarizes the comparisons.

Table 3. Moisture Diffusion Coefficient α from Different Sources.

Source	Estimated α (cm^2/sec)
TAMU Laboratory Measurement Average	3.1×10^{-5}
Australian Experience *(3)*	$3.5 \times 10^{-5} – 4.4 \times 10^{-5}$
Empirical (Eqs. 7 & 8 and Figure 2)	2.4×10^{-5}
Paris Clay Failures (average 16 cases)	$1.3 \times 10^{-5*}$
Beaumont Clay Failures (average 18 cases)	$0.47 \times 10^{-5*}$

*Back-calculated from slope failures.

Some notes on these comparisons are as follows:

- The Australian data *(3)* were on soils identified as expansive clays, but index properties were not reported.
- The empirical estimates are based on a liquid limit of 61, a plasticity index of 39, a fines content (percent Fines) of 74 percent, and a clay fraction of 40 percent. For these data, Eq. 9 estimates the slope of the suction-water content curve (S) to be –10.3. For this exercise, a

typical void ratio value of a high plasticity clay was taken as e=0.83. Using this void ratio with the PI and CF values estimated above, Figure 2 estimates the saturated permeability to be k_0 = 7.6 x 10^{-9} cm/sec. Finally, for S = -10.3, k_0=7.6 x 10^{-9} cm/sec, h_0=200 cm, and a ratio water unit weight to soil dry unit weight (γ_w/γ_d) equal to 0.68 corresponding to a soil void ratio e = 0.83, Eq. 8 predicts a diffusion coefficient α=2.4 x 10^{-5} cm^2/sec.

- Chapter 4 of this manual will show that the time to failure (t_f) for a shallow slope failure is related to the depth of the slide mass (L) and the moisture diffusion coefficient α. For case histories with known failure times and slide mass depths, the analysis can be inverted to estimate the diffusion coefficient α (= $0.3L^2/t_f$). Tables 4 and 5 summarize the data from case histories by Kayyal and Wright (*11*) using this approach from 16 slope failures in Paris clays and 18 slope failures in Beaumont clays. Interpretation of field data necessarily requires that some assumptions regarding the field conditions during the moisture diffusion process prior to slope failure. One of the more critical assumptions was that the surficial cracks occurred immediately following construction, while it is more likely that the cracking process took place over a number of years. The effect of this assumption is that moisture diffusion times should be considered as upper bound estimates and, correspondingly, the reported moisture diffusion coefficients considered as lower bound estimates.

Keeping in mind that the values back-calculated from slope failures are lower bound estimates, Table 3 indicates that a reasonable estimate of the diffusion coefficient α for high plasticity clays is in the range 1 x10^{-5} to 5x10^{-5} cm^2/sec.

Data Evaluation

Regardless of whether α is estimated from empirical correlations or from laboratory measurements, engineering judgment should be applied to evaluate whether the estimated value is reasonable. A good guide is comparison to the saturated diffusion parameter, the coefficient of consolidation (c_v). The parameter (c_v) provides a useful benchmark, since it can be measured conveniently in a standard consolidation test or reliably estimated from empirical correlations *(10)*. Recent studies by Aubeny and Lytton (publication in progress) show the unsaturated diffusion coefficient (α) to be one to two orders of magnitude lower than the saturated value.

Table 4. Diffusion Coefficients Inferred from Paris Clay Slope Failure Data (11).

Depth of Slide Mass (ft)	Time to Failure (yrs)	Estimated α (ft^2/yr)	Estimated α (10^{-5} cm^2/sec)
3.80	19	0.23	0.67
3.71	14	0.30	0.87
7.56	18	0.95	2.81
5.65	18	0.53	1.57
9.38	18	1.47	4.32
3.67	19	0.21	0.63
5.65	18	0.53	1.57
5.50	18	0.51	1.49
4.74	18	0.38	1.11
3.75	18	0.23	0.69
1.91	19	0.061	0.18
3.75	19	0.22	0.66
5.50	19	0.48	1.41
5.50	19	0.48	1.41
3.80	19	0.23	0.67
3.75	19	0.22	0.66

Table 5. Diffusion Coefficients Inferred from Beaumont Clay Slope Failure Data (11).

Depth of Slide Mass (ft)	Time to Failure (yrs)	Estimated α (ft^2/yr)	Estimated α (10^{-5} cm^2/sec)
3.25	17	0.19	0.55
4.08	31	0.16	0.47
2.28	31	0.050	0.15
3.36	31	0.11	0.32
3.73	20	0.21	0.60
2.85	20	0.12	0.36
4.62	20	0.32	0.94
2.38	20	0.085	0.25
2.71	17	0.13	0.38
1.88	19	0.056	0.16
4.69	18	0.37	1.08
4.67	25	0.26	0.77
2.85	14	0.17	0.51
3.33	14	0.24	0.70
2.32	12	0.13	0.40
1.90	18	0.060	0.177
2.77	24	0.096	0.28
3.33	22	0.151	0.45

CHAPTER 4:
SLOPES

This chapter presents suction versus time predictions for relatively simple uniform soil profiles. Slope failures associated with matric suction loss and strength degradation due to moisture infiltration have been overwhelmingly shallow slides that seldom extend to depths more than 8 ft. The depth of moisture infiltration into the slope is small relative to the length of the slope; hence, the slope can be idealized as an infinite slope for which analytical solutions are possible. For the infinite slope case, with no evaporation or infiltration into the slope, the factor of safety against sliding is as follows:

$$FS = \left(\frac{\gamma_b}{\gamma}\right)\frac{\tan\varphi'}{\tan\beta} - \frac{h_{m0}\tan\varphi'}{\gamma H \sin\beta\cos\beta} - \sqrt{2/3}\, a_f \tan\varphi' \qquad \text{(Eq.14)}$$

where FS = factor of safety

γ_b = buoyant unit weight of soil

γ = total unit weight of soil

ϕ' = internal friction angle

β = slope angle

h_{m0} = matric suction at surface

H = vertical depth of slide mass

a_f = Henkel pore pressure coefficient (if undrained shearing occurs)

The formulation of Eq. 14 takes into account soil suction, hydrostatic effects, soil overburden effects, and shear-induced pore pressures. Failures generally occur when the matric suction at the slope surface declines to a level of about 2 pF (h_{m0} = 205 psf). Simple calculations for an infinite slope will show that when the matric suction declines to a level of about 2 pF in slopes ranging from 2.5H:1V to 4H:1V, failure will occur, with the depth of the slide mass being between about 3 to 8 ft.

Given the above scenario, the question arises as to how long it will take for moisture along a wetted boundary of the slope to migrate 3 to 8 ft into the soil mass. Based on these time estimates, evaluation of the relative effectiveness of different slope protection strategies can be

made. Analytical predictions were made with two common slope protection designs in mind. The first is a slope with only vegetative cover. In this case, cracking is inevitable during dry seasons. Once cracking has occurred, moisture will enter the crack and create a more or less permanently wetted boundary from which moisture will diffuse into the soil mass. The second design is a slope protected by concrete riprap. In this case, the riprap is assumed to shelter the soil from extreme drying so cracking is largely inhibited, and the soil can be considered as essentially an intact mass. However, moisture infiltrates from the edges and into the joints in the riprap, so a wetted boundary of the slope will exist at the riprap-soil interface. In this case moisture diffusion into the soil mass will occur but at a much slower rate since the short-circuiting created by the cracks has largely been eliminated.

ANALYTICAL PREDICTIONS

The simplest case is that of an intact soil mass. The most realistic practical case corresponding to this condition is that of a riprap-protected slope. In this case, the riprap protects the soil against the wet-dry cycles that lead to the development of cracks, so the soil can essentially be considered as an intact mass. However, practical experience indicates that riprap cannot realistically provide a watertight seal, so moisture infiltration at the interface of the concrete-soil interface should be considered inevitable. Moisture from this wet interface will gradually diffuse into the soil mass. However, since the mass is intact, the rate of infiltration will be quite gradual.

Due to cracking that develops during wet-dry cycles, an intact condition is unlikely to occur in the case of a bare slope or one that is protected only by vegetation. A predictive model for crack depth is beyond the scope of this manual. However, experience with shallow slope failures suggests that realistic crack depths will vary between 3 and 8 ft with an average of about 6 ft. Empirical evidence suggests that the spacing of the cracks in the directions parallel and perpendicular to the strike of the slope will be roughly equal to their depth.

A realistic estimate of matric suction in a compacted embankment immediately after construction is about u_0 = 3.5 to 4 pF. A realistic estimate of the matric suction at the soil-concrete interface is about u_{wet} = 2 pF. Based on these two estimates, analysis of the moisture diffusion process can proceed, and Figure 6 shows the analytical solutions for intact and cracked

soil masses. Suction is expressed in dimensionless form, $U = (u-u_{wet})/(u_0-u_{wet})$. This figure presents suction as a function of a dimensionless time parameter defined by:

$$T = \alpha t / L^2 \qquad \text{(Eq. 15)}$$

where L = any characteristic dimension of length

α = the moisture diffusion coefficient

t = time

For the case of an intact slope, L should be taken as the distance measured from the slope surface to the point of interest in the soil mass (Figure 7). For the case of a cracked soil mass, L should be taken as the maximum depth of the cracks, normally between 3 and 8 ft (Figure 8).

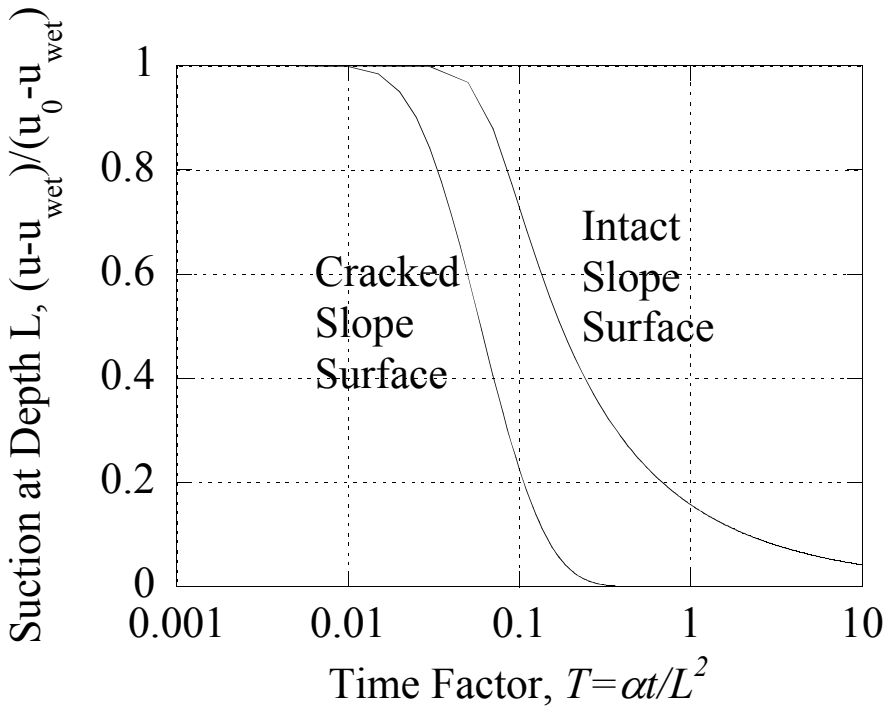

Figure 6. Matric Suction Versus Time in Intact and Cracked Slope Surfaces.

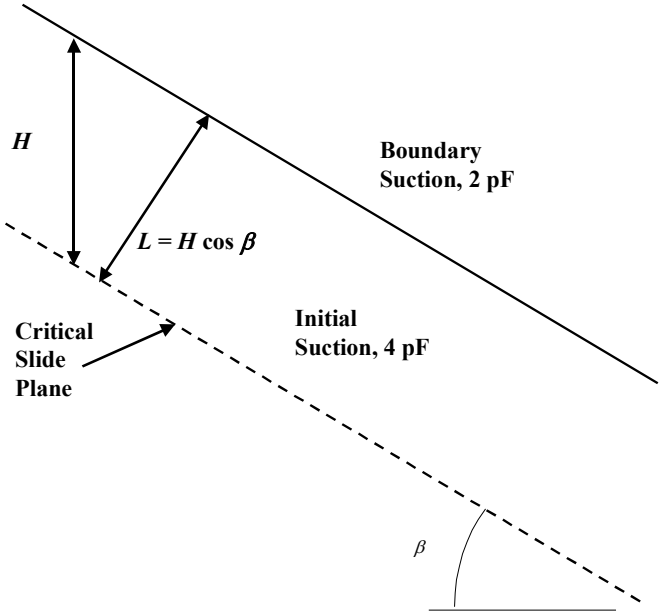

Figure 7. Definition Sketch for Moisture Diffusion into Intact Slope.

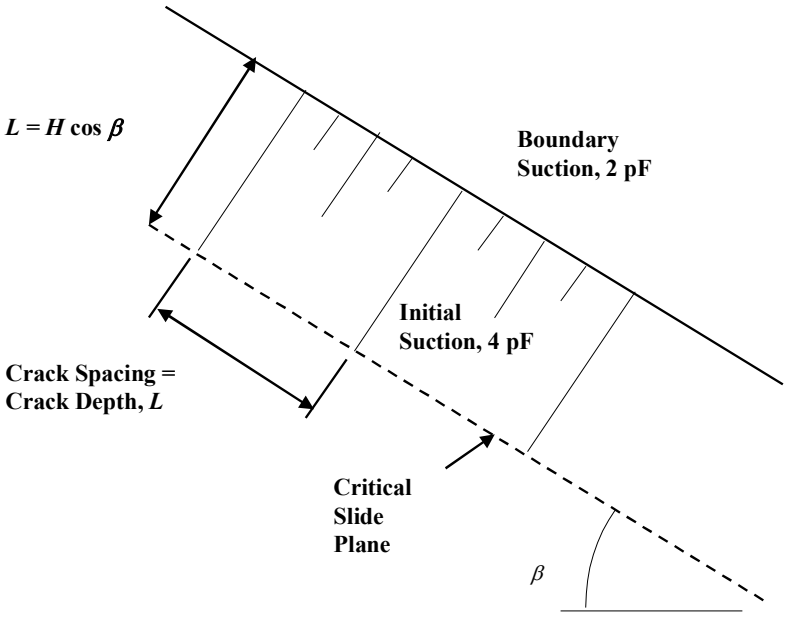

Figure 8. Definition Sketch for Moisture Diffusion into Cracked Slope.

TIME TO FAILURE

Examination of Figure 6 shows that the rate of suction decline in intact slopes is much slower – at least by one order of magnitude – than that in a cracked slope. This implies that although riprap slope protection does not prevent moisture diffusion into the soil mass in a slope, by inhibiting the development of cracks, it does greatly reduce the rate of moisture diffusion into the soil mass. Hence, while not eliminating the possibility of failure due to suction loss and strength degradation, it does greatly defer the time at which problems are likely to occur. From this standpoint, a riprap slope protection provides considerable benefit in protecting the slope.

With regard to real time to slope failures, some estimates can be made based on the following considerations:

- The slide depths typically occur between 3 and 8 ft, so L=3-8 ft.
- A typical diffusion coefficient α is 0.6 ft^2/yr (= $1.7x10^{-5}$ cm^2/sec in Figure 5).
- The time factor T at which the matric suction degrades to its lowest level (2 pF) for the case of a cracked slope is about T=0.3.
- Solving Eq. 15 for real time t yields estimated times to failure of 5 to 30 years. These estimated times are in good accord with actual experience.

The predicted time to failure in an intact (e.g., riprap-protected) slope would be at least 10 times that for a cracked slope. However, a caution should be made about over-confident reliance on riprap protection. If improper attention is given during construction, a perfectly intact condition is unlikely to exist. For example, if the surface is exposed to drying prior to placement of the riprap, some desiccation cracking of the soil mass is likely to occur. Recalling that the benefit of the riprap is that it inhibits cracking associated with wet-dry cycles in the soil, any cracking that is allowed to occur during construction runs counter to that purpose. Nevertheless, if reasonable care is taken during construction not to build cracks into the embankment, riprap protection can greatly defer, if not totally avoid, future strength degradation and stability problems.

Shallow slides occur near the bottom of the cracked zone, or very close to it. Therefore, the analytical solution for suction degradation in a cracked slope (Figure 6, Cracked Slope Surface) is the most appropriate basis for estimating time at which a shallow slide will occur in an unprotected slope. If an estimate of suction decline is required for the intact soil at greater depths within the embankment, a reasonable approach is as follows:

- Estimate the depth of cracking in the embankment. Based on past performance of slopes, a depth of 8 ft is a reasonable high-end estimate.
- Consider the base of this crack zone (i.e., 8 ft below the slope surface) as the boundary condition for the intact moisture diffusion analysis. That is, apply the solution for an intact slope surface in Figure 6 to an imaginary slope surface coinciding with the base of the crack zone.

This procedure obviously neglects the two-dimensional effects associated with moisture infiltrating through an irregular system of cracks into an intact soil mass. However, given the other uncertainties in the problem - the geometry of the crack patterns, the actual amount of surface moisture that actually enters the cracks, and the magnitude of α - this approach should give a reasonably realistic estimate of suction loss in the intact soil region.

CHAPTER 5:
RETAINING STRUCTURES

This chapter presents analytical predictions for suction changes over time for a typical TxDOT earth-retaining structure based on finite element analyses of moisture diffusion into the soil mass.

TYPICAL DESIGNS

Figure 9 shows a typical TxDOT earth-retaining structure. Components of the retaining structure relevant to the moisture diffusion analysis include the wall elements, the pavement, drain material zones adjacent to the wall elements, and the compacted earthfill. A typical height of such a structure is about 20 ft. For the purpose of the analyses, the width of the compacted earthfill portion of the structure, rather than the total width of the structure, influences the moisture infiltration. Therefore the width (W) in the analyses refers to the width of earthfill. Moisture diffusion analyses presented later in this chapter are for structure aspect ratios (W/H) of 4:1 and 8:1.

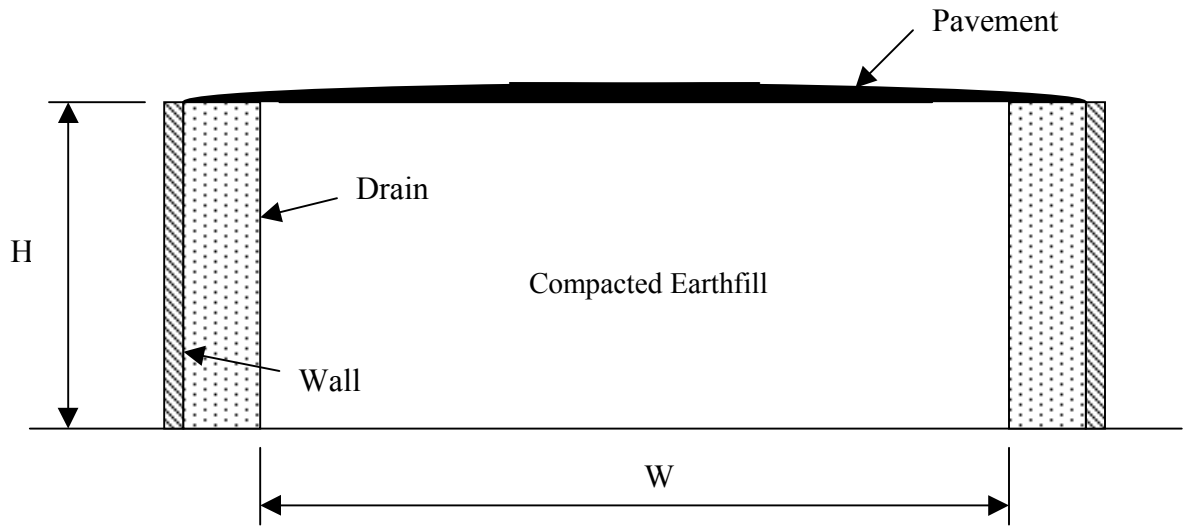

Figure 9. Typical TxDOT Earth-Retaining Structure.

Due to joints and cracking, the pavements are considered to provide imperfect barriers to moisture diffusion. Due to the random nature of cracking and moisture infiltration, the precise

mechanism of moisture infiltration through the pavement was not modeled. Instead it was assumed a priori that wetting would occur at the interface between the pavement and the subgrade soil, and analyses were performed assuming matric suctions at this interface ranging from 2 pF to 3 pF. Experience with removal of existing pavements typically shows that such wetting of soils beneath the pavement indeed occurs. Moisture can also enter the soil mass through the highly permeable drainage zones adjacent to the walls. A reasonable simplifying assumption in the analyses is that the suction at the drain-earthfill interface equals the suction at the pavement-earthfill interface. Natural subgrade soils were assumed to have moisture diffusion properties similar to the compacted clay.

BOUNDARY CONDITIONS

The amount of strength degradation due to moisture infiltration will depend on the boundary conditions, which in turn depend on local soil and climactic conditions. Typical boundary conditions are shown in Figure 10. To provide reasonable first-order estimates of these conditions, this manual considers the three regions of Texas with the eastern region being the wettest and the western being the driest.

Moisture can enter a compacted earthfill through a number of sources. One source of moisture is the natural soils comprising the foundation of the earthfill structure. Since compacted earthfill is usually compacted at lower moisture than the underlying foundation soils, the resulting suction differential will cause moisture to wick up from the foundation into the compacted earthfill. If the earthfill is covered by a pavement or riprap slope protection, moisture will usually penetrate these barriers and form a moist zone at the interface with the earthfill. Again, due to the resulting suction differential, moisture will be drawn down from the wet interface soils into the mass of the earthfill. The analyses require specification of the suction in the native soils at the bottom of the moisture-active zone. A good indicator of this equilibrium suction is the Thornthwaite Moisture Index (TMI), which is a measure of the difference between precipitation and evapo-transpiration rates. The wet regions in east Texas have a positive TMI, while dry regions have negative TMI values. For purposes of the analyses presented in this research, east Texas has a TMI greater than 10; central Texas has a TMI between 10 and –20; and west Texas has a TMI less than –20. Equilibrium matric suctions associated with these TMI ranges are shown in Figure 10.

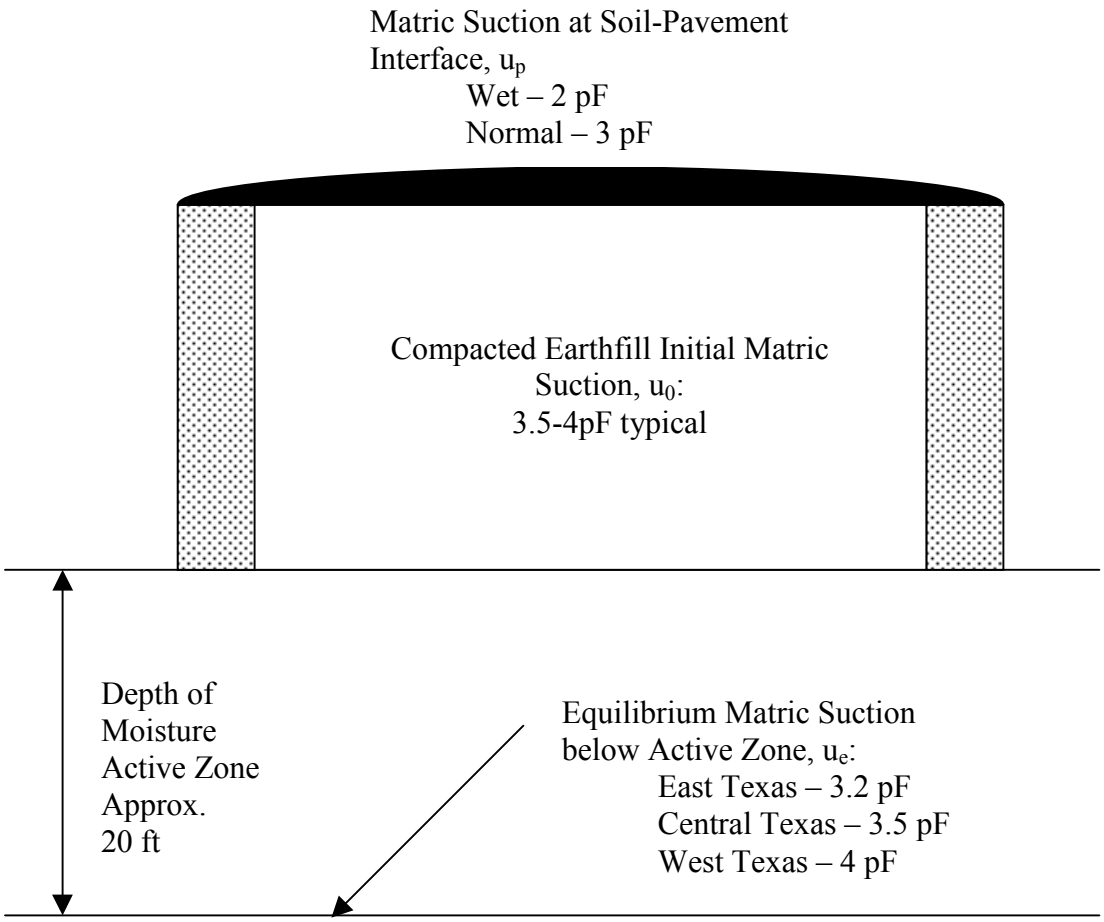

Figure 10. Boundary and Initial Suctions for Moisture Diffusion Analyses.

It should be noted that the moisture and suction in surface soils will vary widely, typically between pF 2.5 to 4.5. With increasing depth, these fluctuations damp out with suction levels remaining relatively constant over time. The active zone refers to the upper zone of fluctuating suction. The suction values cited above for natural soils correspond to conditions in the soils below the active zone.

The boundary conditions listed above are generally appropriate for soils in which the water phase has relatively low salt concentrations with corresponding relatively low levels of osmotic suction. In saline soils, elevated levels of osmotic suction can occur, and special studies will be required to establish appropriate levels of suction.

INITIAL CONDITIONS

In addition to boundary conditions, moisture diffusion analyses require some estimate of initial conditions. An initial matric suction (u_0) of 3.5 to 4 pF is considered reasonable for compacted plastic clays. This is simply a general range based on experience. More reliable estimates of initial suction on a site-specific basis are possible using filter paper test suction measurements on either soil samples collected from the earthfill or on laboratory-compacted specimens.

The analyses assume that the initial matric suction in the sub-grade soil equals the equilibrium suction u_e at the bottom of the moisture-active zone.

MOISTURE DIFFUSION FOR TYPICAL SELECTED CASES

This section presents the numerical analyses for matric suction change versus time. The definition sketch for the coordinate system used in the analyses is shown in Figure 11. Some points to note in using the solutions presented in Figures 12 through 23 are as follows:

- The x-coordinate is measured from the centerline of the earth-retaining structure. The y-coordinate is measured from the bottom of the pavement. The structure is assumed to be symmetric, so predicted suctions in the left half of the structure will be a mirror image of those in the right half. Horizontal and vertical dimensions are normalized by the height of the wall H; i.e., x/H and y/H.
- Predicted suction profiles are presented along horizontal cross-sections at the bottom, quarter, half, and three-quarter elevations of the wall: y/H = 0.25, 0.5, 0.75, and 1.0.
- A dimensionless time factor T is defined as:

$$T = \alpha\, t / H^2 \qquad \text{(Eq. 16)}$$

where t = real time

α = the moisture diffusion coefficient of the clay

H = the height of the structure

- Computations can proceed in any units provided that they are consistent. For example, if the height of the wall is expressed in ft and real time is expressed in years, the moisture diffusion coefficient α must be expressed in ft^2/yr.

- Matric suction is expressed in terms of a dimensionless term (U)

$$U = (u-u_p) / (u_e-u_p) \quad \text{(Eq. 17)}$$

where u = matric suction at time (t)

u_p = the user-specified matric suction at the pavement-earthfill interface

u_e = equilibrium matric suction at bottom of moisture-active zone

- The initial matric suction in the compacted earthfill is characterized by a parameter (U_0)

$$U_0 = (u_0-u_p) / (u_e-u_p) \quad \text{(Eq. 18)}$$

where u_0 is the initial matric suction in the compacted earthfill. Solutions are presented for (U_0) values of 5, 4, 3, 2, 1, and 0.5.

- Solutions are presented for retaining structure width-to-height ratios (W/H) of 4 (Figures 12 through 17) and 8 (Figures 18 through 23).

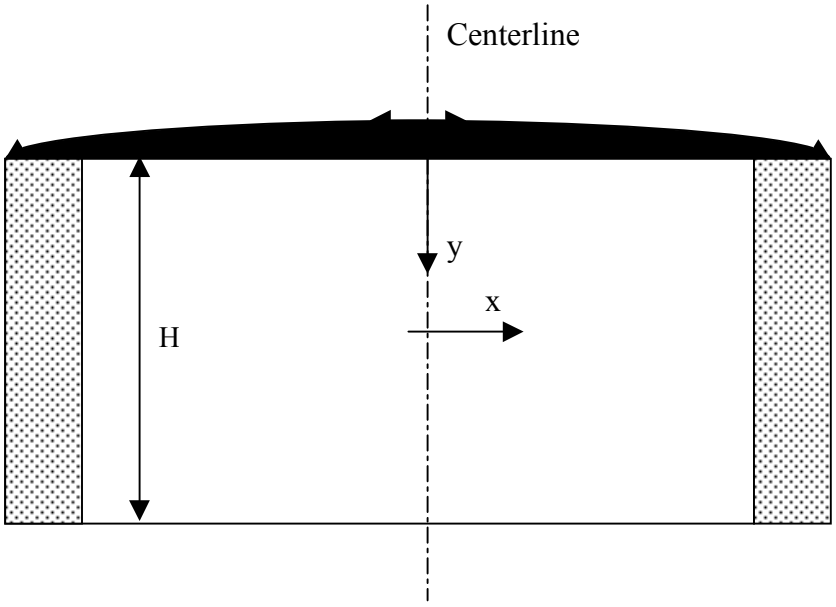

Figure 11. Definition Sketch for Suction Predictions.

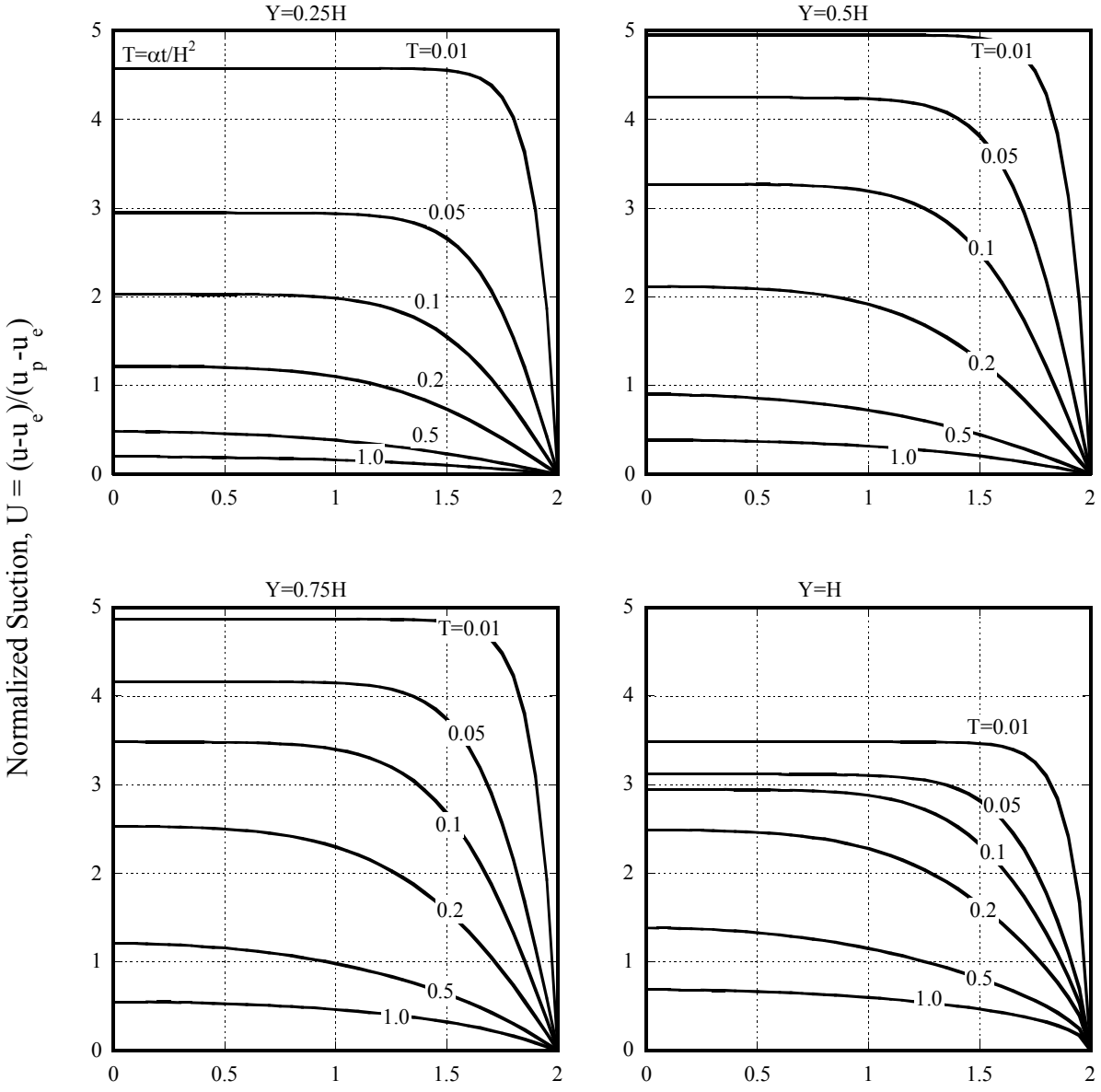

Figure 12. Suction versus Time for Structure with Aspect Ratio 4H:1V and U_0=5.

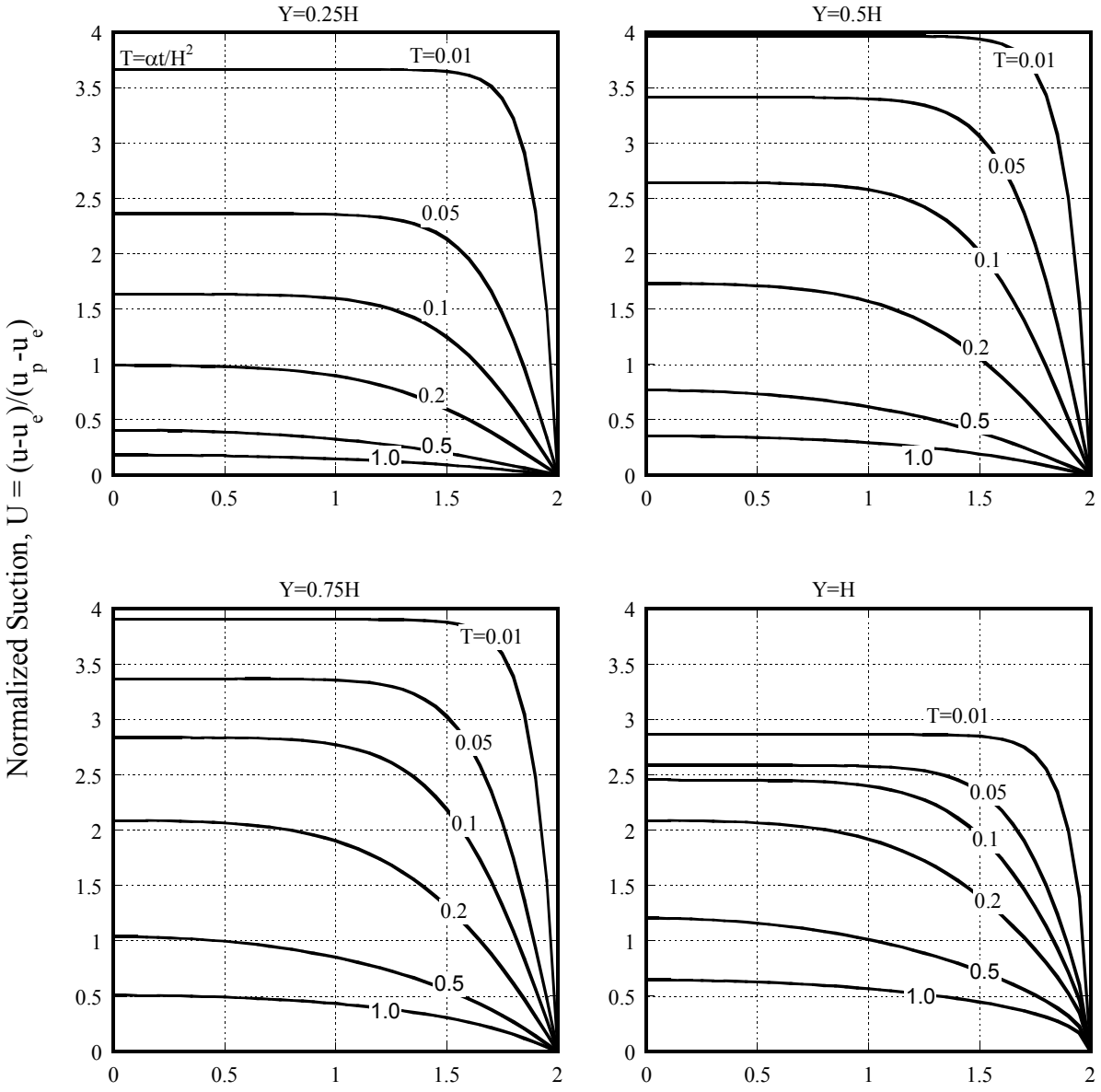

Figure 13. Suction versus Time for Structure with Aspect Ratio 4H:1V and U_0=4.

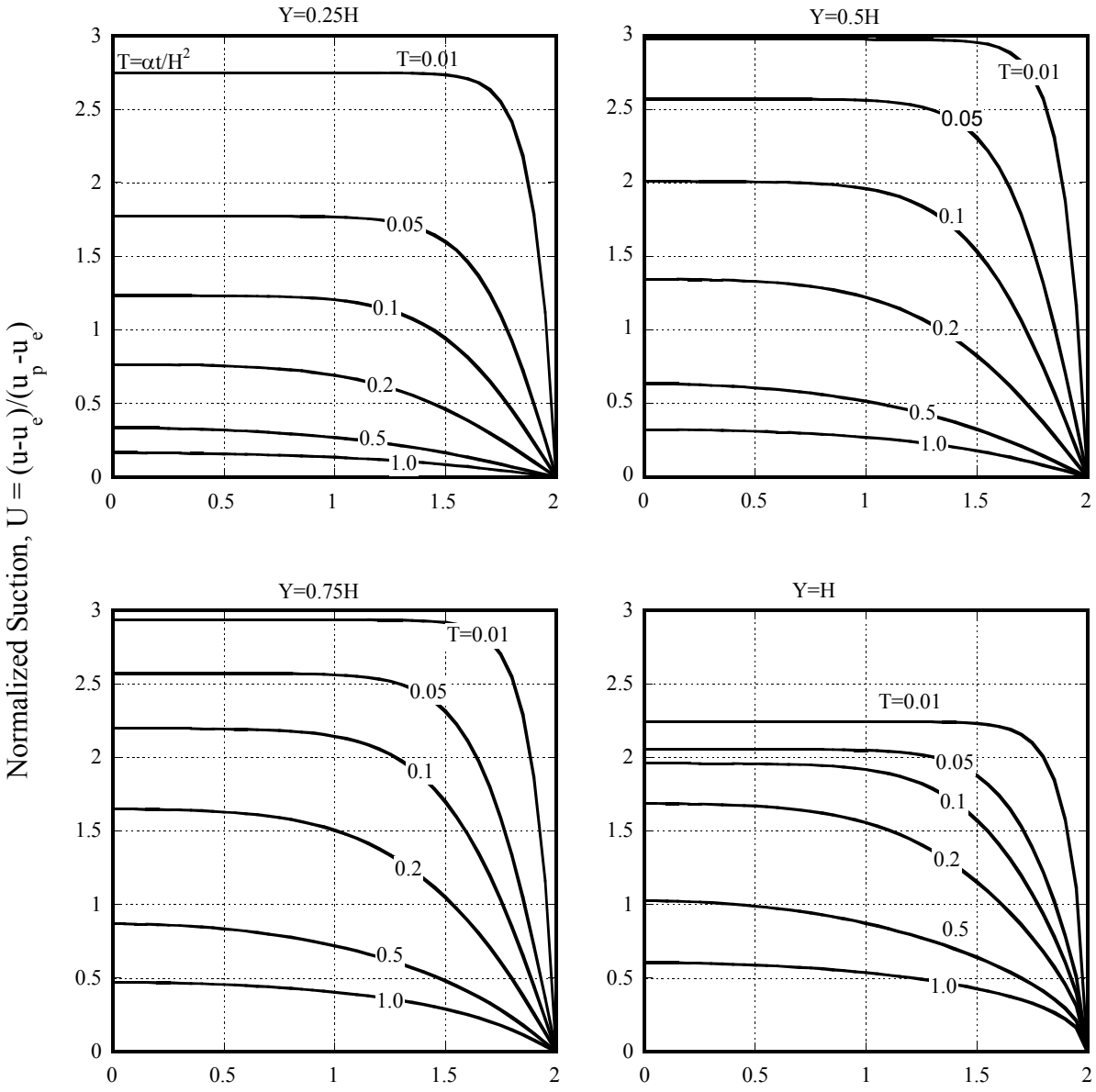

Figure 14. Suction versus Time for Structure with Aspect Ratio 4H:1V and U_0=3.

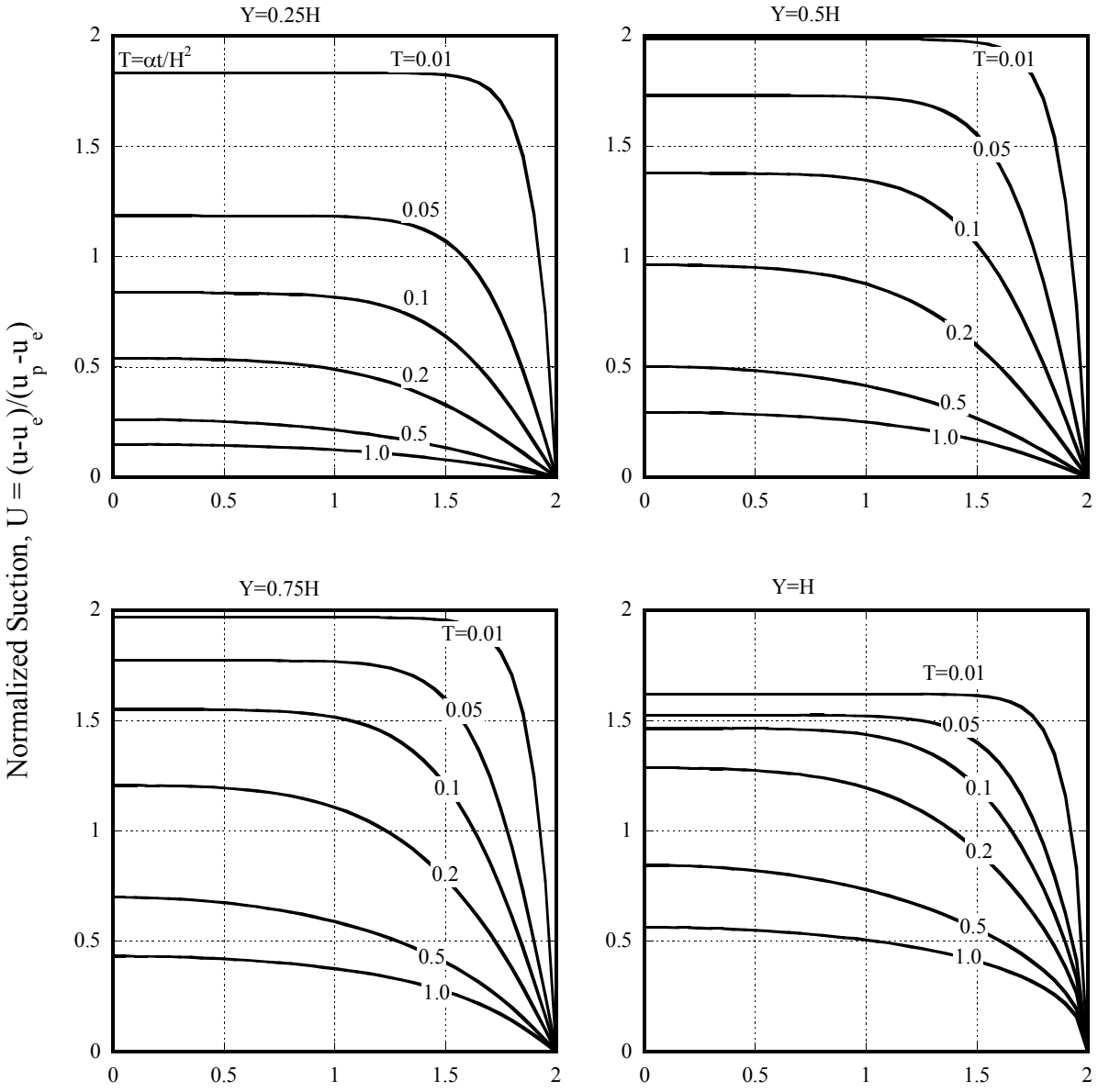

Figure 15. Suction versus Time for Structure with Aspect Ratio 4H:1V and U_0=2.

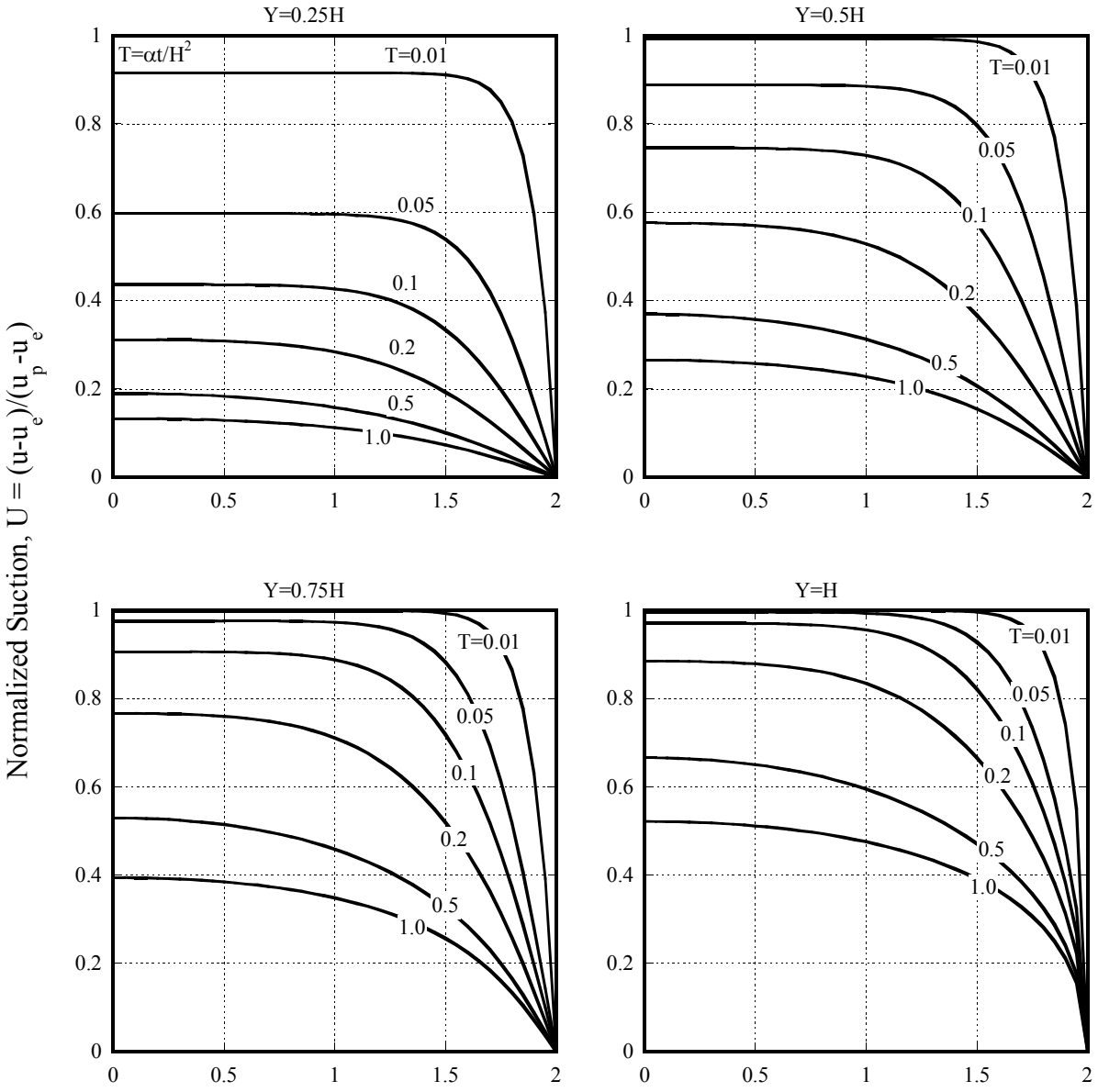

Figure 16. Suction versus Time for Structure with Aspect Ratio 4H:1V and U_0=1.

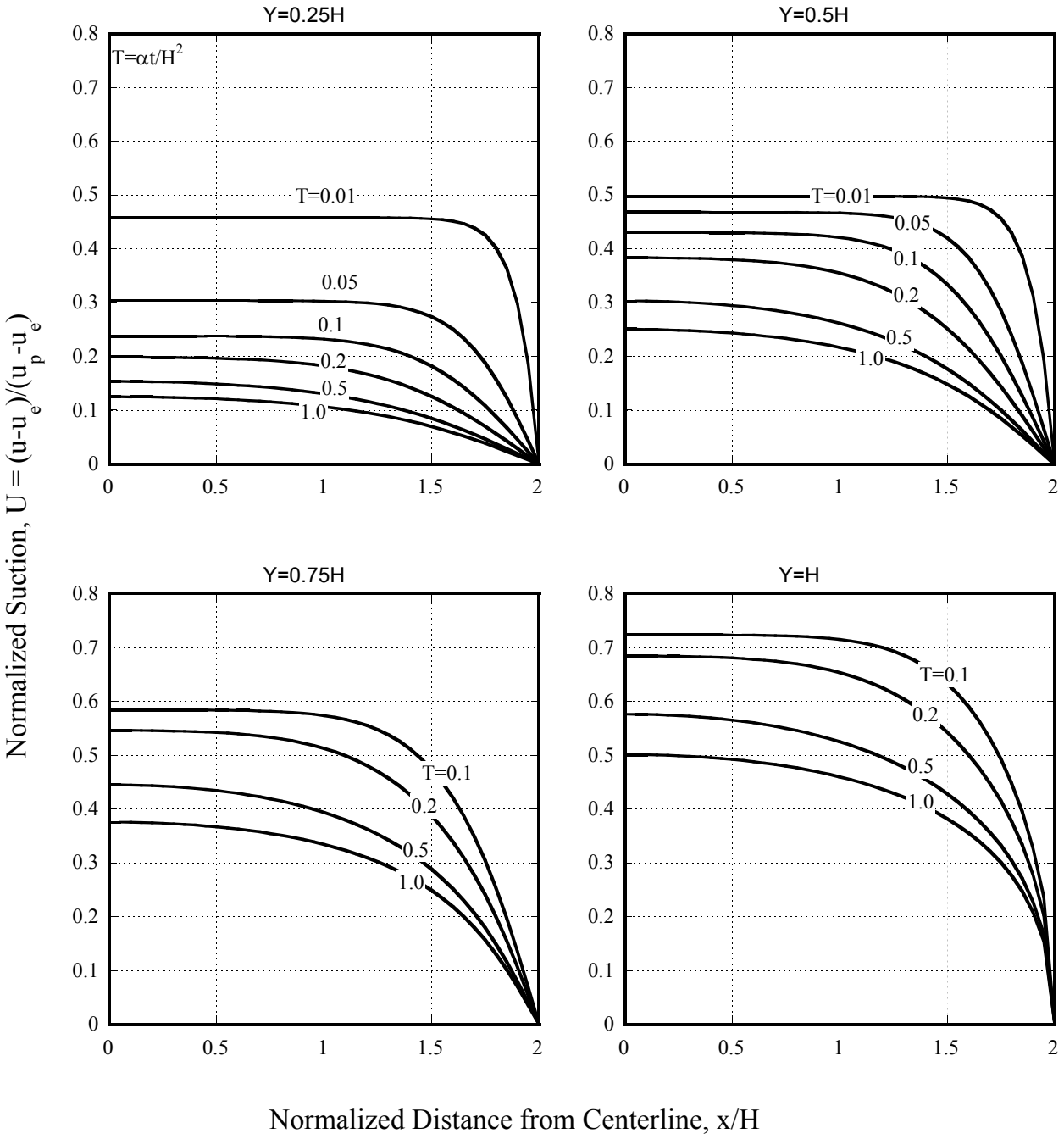

Figure 17. Suction versus Time for Structure with Aspect Ratio 4H:1V and U_0=0.5.

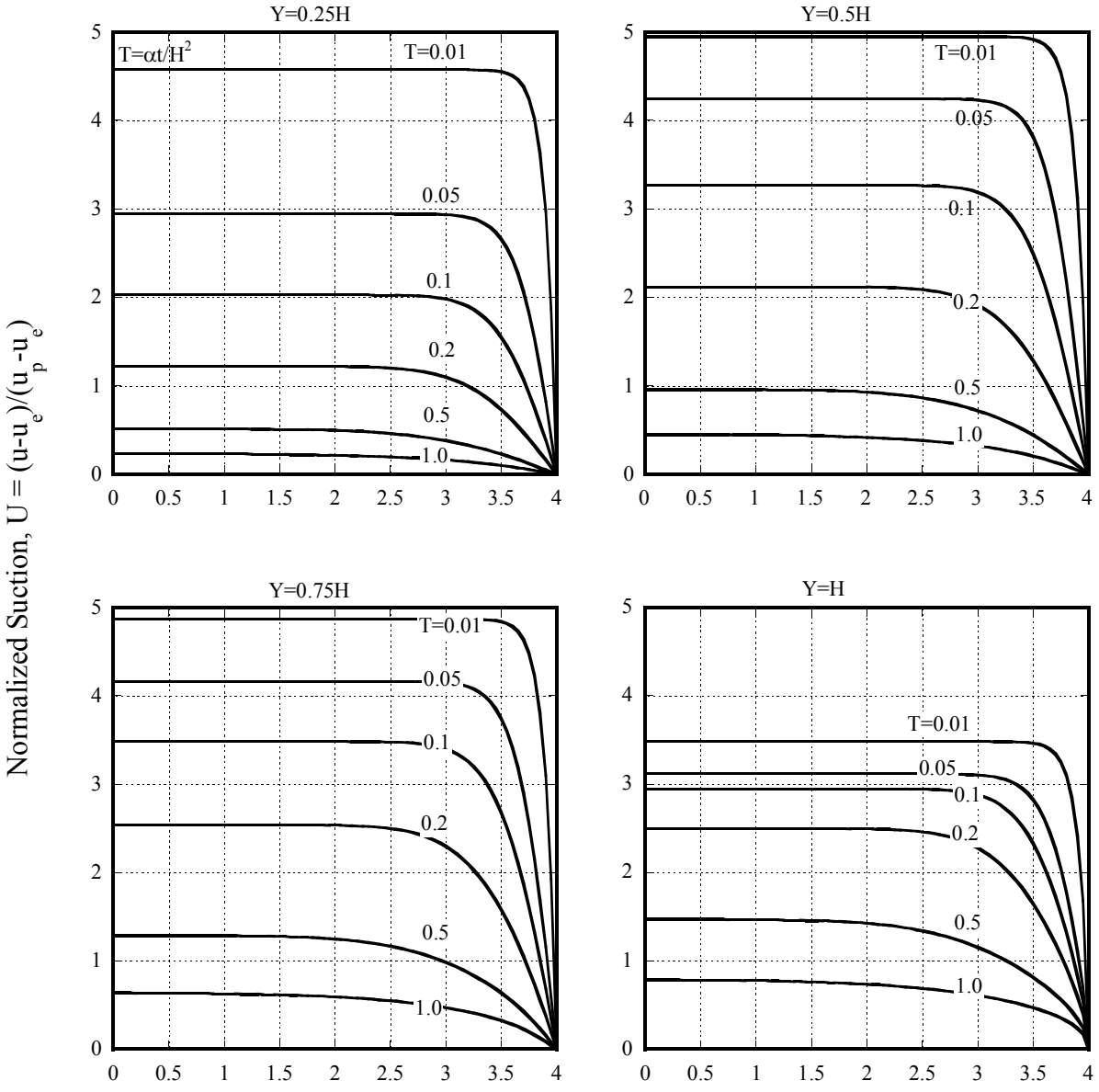

Figure 18. Suction versus Time for Structure with Aspect Ratio 8H:1V and U_0=5.

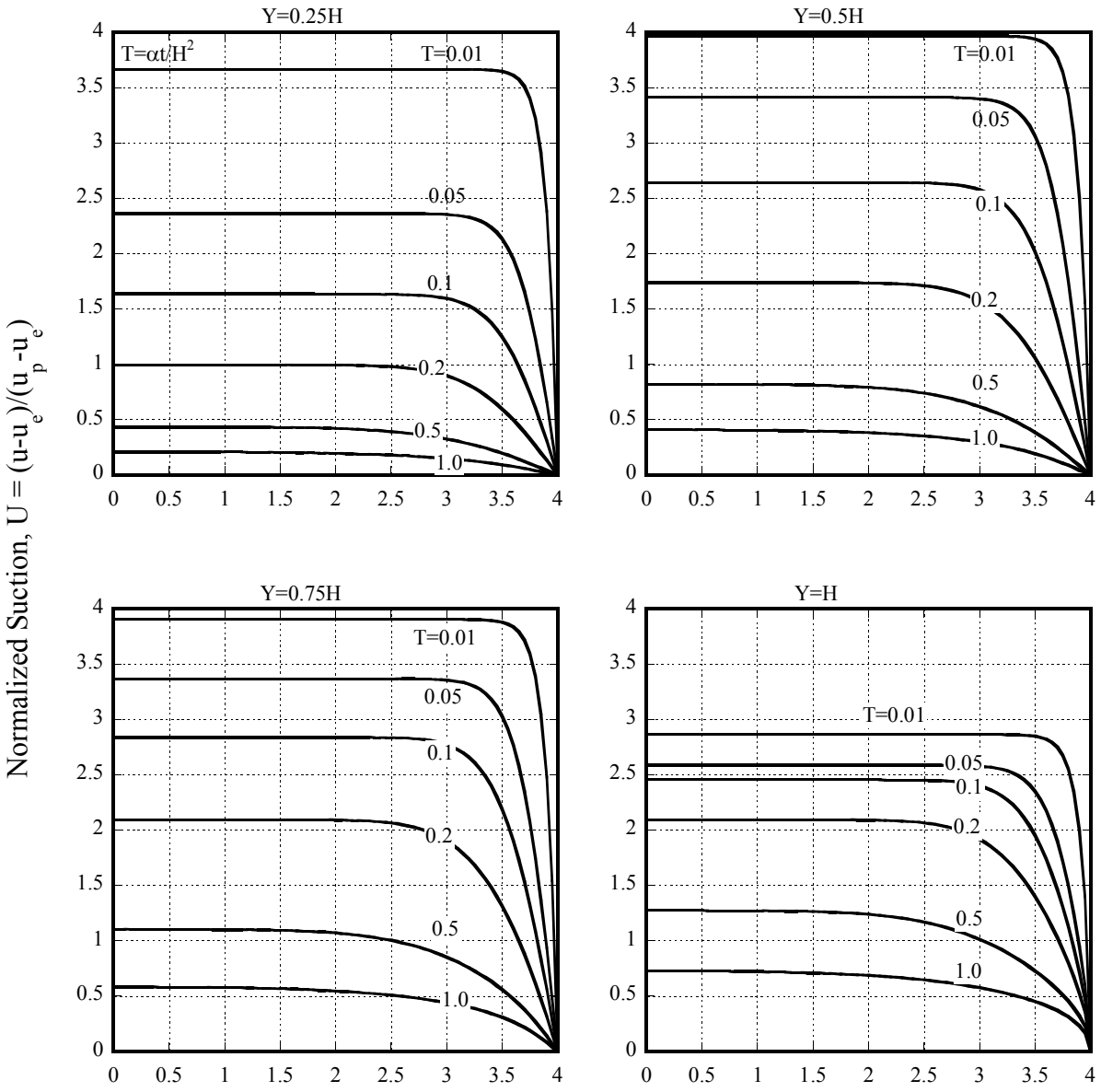

Figure 19. Suction versus Time for Structure with Aspect Ratio 8H:1V and U_0=4.

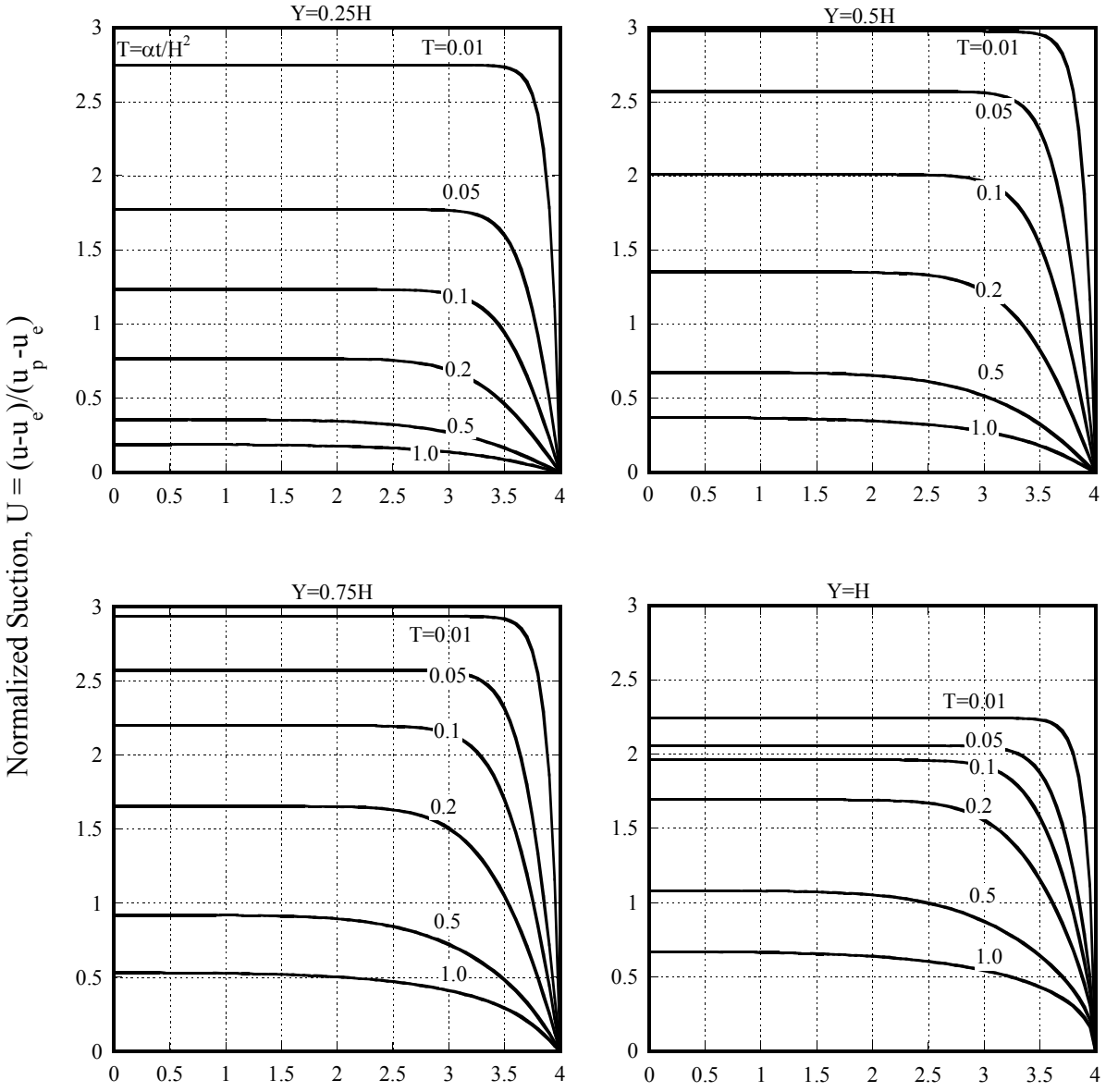

Figure 20. Suction versus Time for Structure with Aspect Ratio 8H:1V and U_0=3.

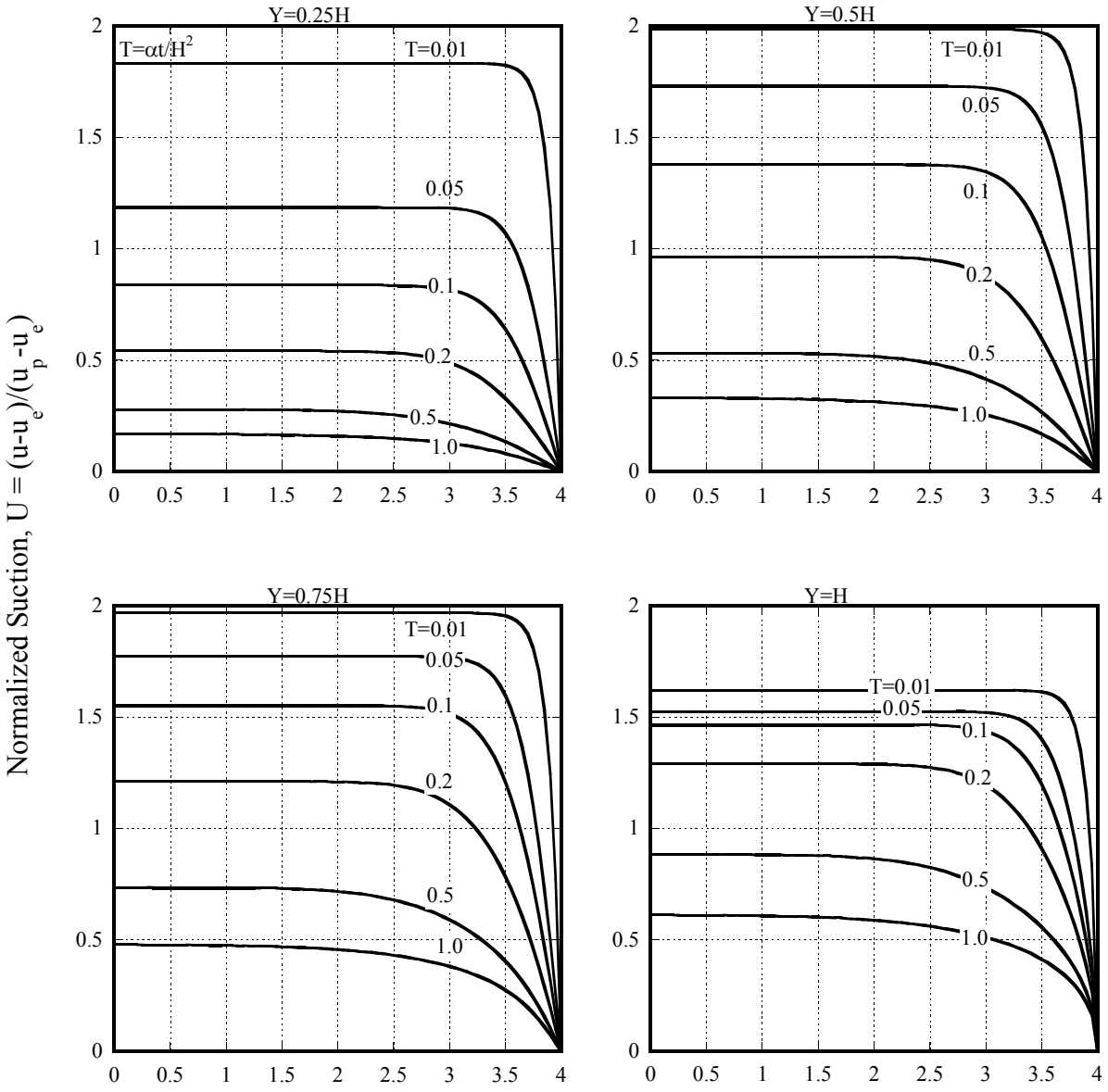

Figure 21. Suction versus Time for Structure with Aspect Ratio 8H:1V and U_0=2.

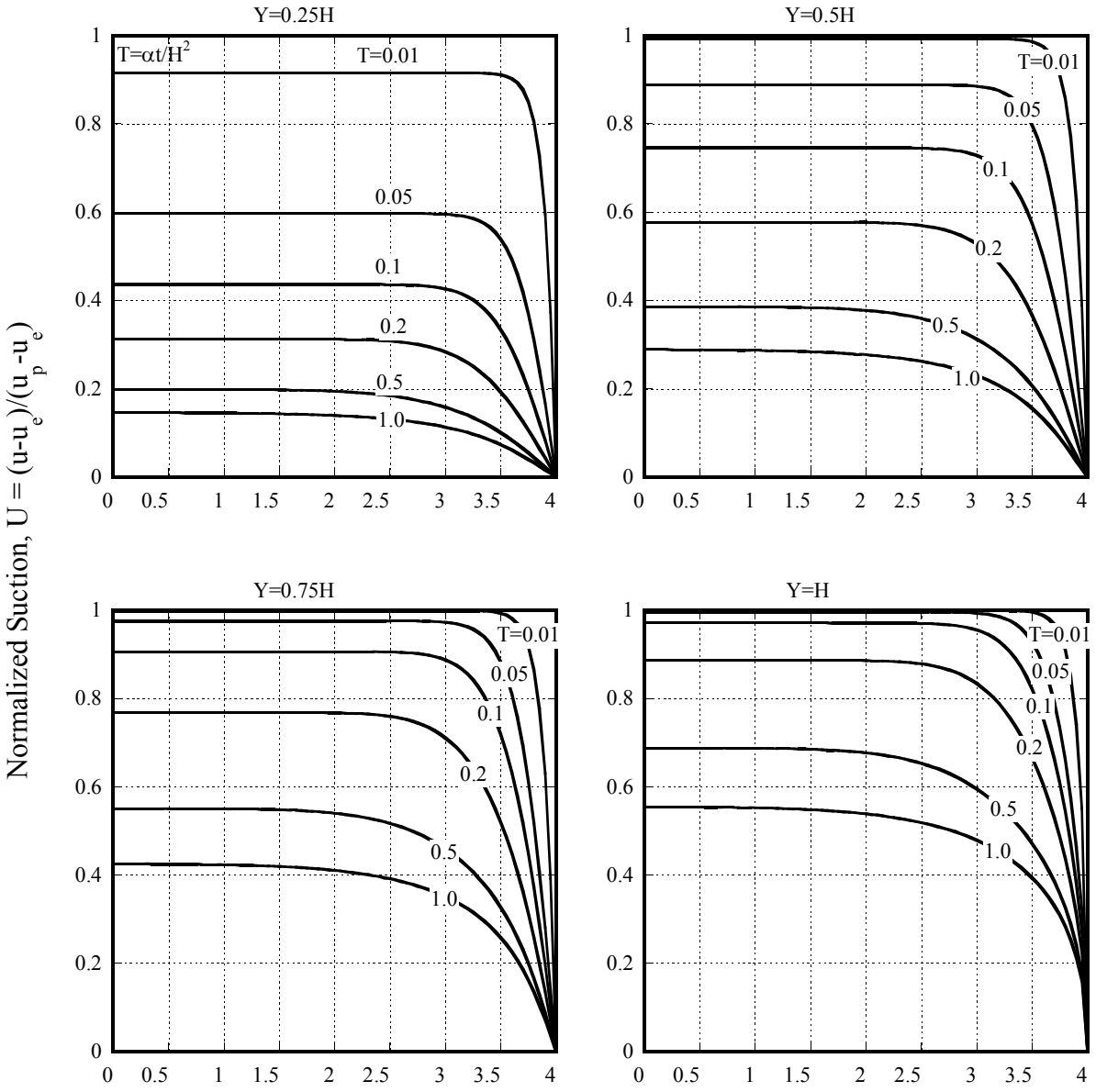

Figure 22. Suction versus Time for Structure with Aspect Ratio 8H:1V and U_0=1.

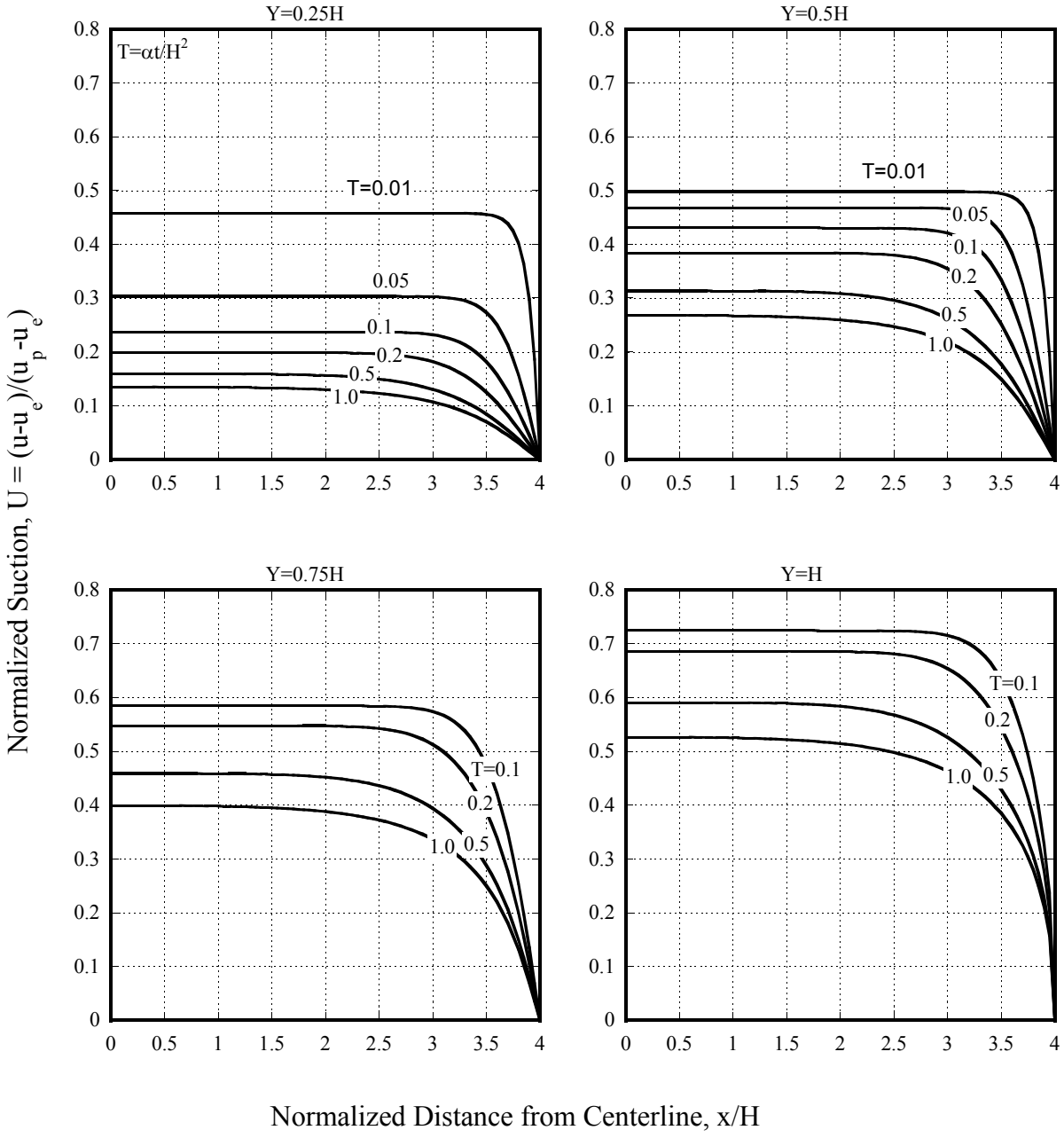

Figure 23. Suction versus Time for Structure with Aspect Ratio 8H:1V and U_0=0.5.

USE OF SUCTION PREDICTION ANALYSES

This section presents an illustrative example of how the predicted suction versus time relationships in Figures 12 through 23 may be used to compute soil strength changes over time. The analyses will focus on computation of the apparent cohesion (c_{app}). This apparent cohesion can be used in the normal Mohr-Coulomb equation, which can in turn be utilized in conventional slope stability, earth pressure, and bearing capacity analyses.

The example problem considers an earth-retaining structure 20 ft high with the width of the compacted earthfill (see Figure 9) being 80 ft. The compacted clay has the following properties:

ϕ' = 26 degrees

α = $3x10^{-5}$ cm^2/sec

γ_d = 93 lb/ft^3

w = 24.2 percent

G_s = 2.7

The reader is referred to Eq. 5 for empirically estimating the friction angle ϕ' and to Eq. 8 for estimating the diffusion coefficient α.

At a point located 30 ft from the centerline at the mid-depth of the structure, estimate the strength of clay (a) as-compacted, (b) after 20 years, and (c) after 40 years. Select suction conditions typical of Central Texas; assume that the matric suction in the earthfill at the time of placement is u_0 = 3.5 pF, and assume wet conditions prevail beneath the pavement.

1. *Dimensionless coordinates and times.* To use the charts, coordinates and time must be expressed in dimensionless terms. Coordinates are normalized by the height of the structure (H). Therefore the dimensionless horizontal distance from the centerline is:

   x / H = 30 ft / 20 ft = 1.5

   Since the mid-depth is the point of interest, y = 0.5H.

   The dimensionless time factor T is defined by Eq. 16. Since consistent units must be used, the diffusion coefficient (α) must be converted to units of ft^2/yr. The conversion will show that $3x10^{-5}$ cm^2/sec is equivalent to 1.0 ft^2/yr. The dimensionless time factors for the three times of interest are now as follows:

Real Time (years)	Dimensionless Time, $T = \alpha t/H^2$
0	0
20	0.05
40	0.10

2. *Dimensionless Initial Suction, U_0.* Predictions of suction require estimates of the suction beneath the pavement (u_p), the equilibrium suction at the bottom of the moisture-active zone in the sub-grade soil (u_e), and the matric suction in the compacted soil (u_0).

   - Suction beneath pavement (u_p): The problem specified that wet conditions should be assumed to prevail beneath the pavement. From the recommendation provided earlier in this chapter, wet conditions would correspond to a matric suction $u_p = 2$ pF.
   - Equilibrium suction (u_e): From the recommendation provided earlier in this chapter, a reasonable estimate of the equilibrium matric suction in Central Texas is $u_e = 3.5$ pF.
   - Initial suction in earthfill (u_0): The problem specified an initial matric suction in the compacted earthfill $u_0 = 3.5$ pF.

   Based on these three suction values, the normalized suction value (U_0) for use in the charts is:

   $$U_0 = (u_0 - u_p) / (u_e - u_p) = (3.5 - 2) / (3.5 - 2) = 1$$

   For a U_0 value of 1.0 in a retaining structure having a 4H:1V aspect ratio, the appropriate chart is found in Figure 16.

3. *Suction versus Time from Charts.* Entering Figure 16 for x / H = 1.5, and T = 0, 0.05, and 0.1, yields the dimensionless suction values shown in the table below. Dimensionless suction from the chart is converted to real suction as follows:

   $$u = U (u_e - u_p) + u_p$$

   For use in strength calculations, the suction in pF must be converted to units of pressure. Finally, the hydrostatic pressure due to the column of water above the point in question should be added to the computed matric suction. This hydrostatic pressure correction

should be made for any case in which the water in the soil voids is continuous; i.e., for suction magnitudes less than 3.5 pF.

T	U (Figure 15)	Suction, u (pF)	Suction, h_m (psf)	Hydrostatic Correction (psf)	Corrected Suction, h_{mc} (psf)
0	1.0	3.5	-6,470	620	-5,850
0.05	0.80	3.20	-3,240	620	-2,620
0.10	0.57	2.86	-1,480	620	-860

4. *Apparent Cohesion from Suction.* With the suctions estimated, unconfined shear strength (C_{uc}) calculations can proceed using Eq. 4. Chapter 2 presents example strength calculations in great detail; therefore, all details are not repeated here. The table below summarizes the main calculations.

Time (years)	Suction (pF)	Gravimetric Moisture, w (percent)	Saturation, S (percent)	Volumetric Moisture Θ (percent)	f	Corrected Suction, h_{mc} (psf)	Unconf. Shear Strength C_{uc} (psf)
0	3.50	27.2	90.6	40.5	1.55	-5,850	2,870
20	3.20	27.9	93.0	41.6	1.75	-2,620	1,490
40	2.86	28.7	95.7	42.8	1.95	-860	560

REFERENCES

1. Mitchell, J.K. (1976) *Fundamentals of Soil Behavior*, John Wiley and Sons, New York, 422 pages.

2. Lamborn, M.K. (1986) *A Micromechanic Approach to Modeling Partly Saturated Soils*, Master of Science Thesis, Texas A&M University, College Station, Texas.

3. Mitchell, P.W. (1979) "The Structural Analysis of Footings on Expansive Soils," Research Report No. 1, K.W.G. Smith and Assoc. Pty. Ltd., Newton, South Australia.

4. Jayatilaka, R. and R.L. Lytton (1999) "Prediction of Expansive Clay Roughness in Pavements with Vertical Moisture Barriers," Research Report No. FHWA/TX-98/197-28F, Texas Transportation Institute, College Station, Texas.

5. Tavenas, F., P. LeBlond, and S. Leroueil (1983) "The Permeability of Natural Soft Clays. Part II, Permeability Characteristics", Canadian Geotechnical Journal, Vol. 20, No. 4, pp. 645-660.

6. Covar, A.P. and R.L. Lytton (2001), "Estimating Soil Swelling Behavior Using Soil Classification Properties", ASCE Geotechnical Special Technical Publication No. 115, pp. 44-63.

7. Aubeny, C., R.L. Lytton, and D. Tang (2003) "Simplified Analysis of Unsteady Moisture Flow through Unsaturated Soil", *82nd Annual Meeting of Transportation Research Board.*

8. Fredlund, D.G. and H. Rahardjo (1993) *Soil Mechanics for Unsaturated Soils*, John Wiley & Sons, New York.

9. Reynolds, W.C. and H.C. Perkins (1970) *Engineering Thermodynamics*, McGraw-Hill, New York, 585 pages.

10. Naval Facilities Engineering Command (1986) Soil Mechanics, Design Manual 7.01.

11. Kayyal, M.K. and S.G. Wright (1991) Investigation of Long-Term Strength Properties of Paris and Beaumont Clays in Earth Embankments, Research Report 1195-2F, Center for Transportation Research, University of Texas at Austin.